別紙５　研究成果の刊行に関する一覧表

1: Satow R, Shitashige M, Jigami T, Fukami K, Honda K, Kitabayashi I, Yamada T.

β-Catenin inhibits promyelocytic leukemia protein tumor suppressor function in colorectal cancer cells.

Gastroenterology. 2012;142(3):572-81.

2: Ito H, Honda K, Satow R, Arai E, Shitashige M, Ono M, Sakuma T, Sakano S, Naito K, Matsuyama H, Yamada T.

Combined functional genome survey of therapeutic targets for clear cell carcinoma of the kidney.

Jpn J Clin Oncol. 2011;41(7):847-53.

3: Nagashio R, Arai E, Ojima H, Kosuge T, Kondo Y, Kanai Y.

Carcinogenetic risk estimation based on quantification of DNA methylation levels in liver tissue at the precancerous stage.

Int J Cancer. 2011;129(5):1170-9.

4: Nishiyama N, Arai E, Nagashio R, Fujimoto H, Hosoda F, Shibata T, Tsukamoto T, Yokoi S, Imoto I, Inazawa J, Kanai Y.

Copy number alterations in urothelial carcinomas: their clinicopathological significance and correlation with DNA methylation alterations.

Carcinogenesis. 2011;32(4):462-9.

5: Arai E, Nakagawa T, Wakai-Ushijima S, Fujimoto H, Kanai Y.

DNA methyltransferase 3B expression is associated with poor outcome of stage I testicular seminoma.

Histopathology. 2012;60(6B):E12-8.

6: Kikuta K, Kubota D, Saito T, Orita H, Yoshida A, Tsuda H, Suehara Y, Katai H, Shimada Y, Toyama Y, Sato K, Yao T, Kaneko K, Beppu Y, Murakami Y, Kawai A, Kondo T.

Clinical proteomics identified ATP-dependent RNA helicase DDX39 as a novel biomarker to predict poor prognosis of patients with gastrointestinal stromal tumor.

J Proteomics. 2012;75(4):1089-98.

7: Morofuji N, Ojima H, Onaya H, Okusaka T, Shimada K, Sakamoto Y, Esaki M, Nara S, Kosuge T, Asahina D, Ushigome M, Hiraoka N, Nagino M, Kondo T.
Macrophage-capping protein as a tissue biomarker for prediction of response to gemcitabine treatment and prognosis in cholangiocarcinoma.
J Proteomics. 2012;75(5):1577-89.

8: Moroishi T, Nishiyama M, Takeda Y, Iwai K, Nakayama KI.
The FBXL5-IRP2 axis is integral to control of iron metabolism in vivo.
Cell Metab. 2011 Sep 7;14(3):339-51. PubMed PMID: 21907140.

9: Matsumoto A, Takeishi S, Kanie T, Susaki E, Onoyama I, Tateishi Y, Nakayama K, Nakayama KI.
p57 is required for quiescence and maintenance of adult hematopoietic stem cells.
Cell Stem Cell. 2011;9(3):262-71.

10: Onoyama I, Suzuki A, Matsumoto A, Tomita K, Katagiri H, Oike Y, Nakayama K, Nakayama KI.
Fbxw7 regulates lipid metabolism and cell fate decisions in the mouse liver.
J Clin Invest. 2011 Jan;121(1):342-54.

β-Catenin Inhibits Promyelocytic Leukemia Protein Tumor Suppressor Function in Colorectal Cancer Cells

REIKO SATOW,*,‡ MIKI SHITASHIGE,* TAKAFUMI JIGAMI,* KIYOKO FUKAMI,‡ KAZUFUMI HONDA,* ISSAY KITABAYASHI,§ and TESSHI YAMADA*

*Divisions of *Chemotherapy and Clinical Research and §Hematological Malignancy, National Cancer Center Research Institute, Tokyo; and ‡Laboratory of Genome and Biosignal, Tokyo University of Pharmacy and Life Sciences, Tokyo, Japan*

BACKGROUND & AIMS: Loss of promyelocytic leukemia protein (PML) nuclear body (NB) formation has been reported in colorectal and other solid tumors. However, genetic alteration of *PML* is rarely observed in these tumors; the exact mechanisms that mediate loss of PML function are not known. **METHODS:** We previously used a comprehensive shotgun mass spectrometry approach to identify PML as 1 of 70 proteins that coimmunoprecipitate with anti–T-cell factor 4 in DLD-1 and HCT116 colorectal cancer cell lines; we investigated the effects of altered β-catenin expression on PML function in these cells. **RESULTS:** β-catenin specifically interacted with the product of *PML* transcript variant IV (PML-IV) through the armadillo repeat domain of β-catenin. Overexpression of β-catenin in colorectal cancer cells disrupted the subcellular compartmentalization of PML-IV, whereas knockdown of β-catenin restored formation of PML-NB. Modification of PML by the small ubiquitin-related modifier (SUMO) is required for proper assembly of PML-NB. β-catenin inhibited Ran-binding protein 2–mediated SUMOylation of PML-IV. **CONCLUSIONS: β-catenin interacts with PML isoform IV and disrupts PML-IV function and PML-NB formation by inhibiting Ran-binding protein 2–mediated SUMO modification of PML-IV. These findings indicate the involvement of a posttranslational mechanism in disruption of PML-NB organization in cancer cells and provide more information about the oncogenic functions of β-catenin.**

Keywords: Wnt Signaling; Colorectal Cancer; TCF4; PML.

BASIC AND TRANSLATIONAL AT

The majority of colorectal cancers have somatic mutations in the adenomatous polyposis coli (*APC*) gene, and about one-half of those with the wild-type *APC* gene have mutations in the β-catenin (*CTNNB1*) gene.[1–3] Either mutation results in stabilization and accumulation of β-catenin protein. It is believed that accumulated β-catenin exerts its oncogenic function mainly by cotransactivating the target genes of TCF/lymphoid enhancer factor (LEF)-family transcriptional factors.[4] However, β-catenin is a multifunctional protein, and its function varies according to the context of partner proteins with which it forms complexes.[5] Our recent series of proteomics studies has revealed that β-catenin plays various roles in DNA damage recognition,[6,7] pre-messenger RNA splicing,[8,9] and cell motility[10] through interaction with poly (adenosine diphosphate–ribose) polymerase-1, Ku70, FUS/TLS proto-oncogene product, splicing factor 1, and actinin 4.

A previous unbiased analysis of the protein composition of the T-cell factor (TCF) 4 and β-catenin nuclear complex we performed using highly tuned mass spectrometry identified 70 proteins,[11] among which promyelocytic leukemia protein (PML) attracted our current attention. PML is a tumor suppressor that was originally identified in the t(15;17) chromosome translocation site of acute promyelocytic leukemia. This chromosome translocation generates the PML and retinoic acid receptor α fusion protein,[12,13] which acts as a dominant negative mutant for PML and inhibits its tumor suppressor function.[14–16] PML is essential for the formation of the nuclear speckled substructure known as PML-nuclear body (NB). PML recruits a large variety of proteins into PML-NB and mediates various fundamental nuclear functions such as DNA replication, transcription, and epigenetic silencing,[17–22] as well as regulating cell death, proliferation, and senescence.[14,17,19,23,24] Inhibition of PML-NB formation has been considered one of the main mechanisms by which the PML–retinoic acid receptor α fusion protein promotes leukemogenesis.

Loss of the tumor-suppressive function of PML does not seem to be limited to hematologic malignancies. Formation of PML-NB and expression of PML protein are often lost in various human solid tumors including colorectal cancer,[25,26] but mutation or loss of heterozygosity of the *PML* gene has rarely been detected, and expression of PML messenger RNA is well retained in these tumors, indicating that the disruption of PML function is not caused by genetic or epigenetic inactivation of *PML*. However, the precise molecular mechanisms behind the loss of PML function in solid tumors have remained largely unknown.

Here we report the novel posttranslational regulation of PML tumor suppressor function by an oncogene product,

Abbreviations used in this paper: DAPI, 4′,6-diamidino-2-phenylindole; GST, glutathione S-transferase; HA, hemagglutinin; HDAC7, histone deacetylase 7; NB, nuclear body; PML, promyelocytic leukemia protein; RanBP2, Ran-binding protein 2; SDS-PAGE, sodium dodecyl sulfate/polyacrylamide gel electrophoresis; siRNA, small interfering RNA; SUMO, small ubiquitin-related modifier; TCF, T-cell factor.

0016-5085/$36.00
doi:10.1053/j.gastro.2011.11.041

β-catenin. β-catenin physically interacts with PML and inhibits the SUMOylation of PML and subsequent formation of PML-NB. Our data reveal a new aspect of β-catenin function and may provide insights into the molecular mechanisms of colorectal carcinogenesis, as well as suggesting novel forms of therapeutic intervention.

Materials and Methods

Cell Lines

The human embryonic kidney cell line HEK293 and the human colorectal cancer cell lines DLD1 and Lovo were obtained from the Health Science Research Resources Bank (Osaka, Japan). The human colorectal cancer cell line SW48 was purchased from American Type Culture Collection (Rockville, MD). The human cervical cancer cell line HeLa was obtained from Riken Cell Bank (Tsukuba, Japan). Mitomycin C was purchased from Sigma-Aldrich (St Louis, MO).

Plasmids and Small Interfering RNA

pLNCX constructs encoding Flag-tagged human PML isoforms (Flag-PML-I to -IV) were described previously.[27] The human β-catenin complementary DNA (cDNA) lacking the N-terminal casein kinase I/glycogen synthase kinase 3β (CKI/GSK3β)-phosphorylation sites (β-catenin ΔN134)[11] and the full-length human TCF4 (splice form E) cDNA[28] were subcloned into pCIneo-hemagglutinin (HA) (Promega, Madison, WI). Ran-binding protein 2 (RanBP2) cDNA was subcloned into pcDNA3.1 as described previously.[11] pcDNA3.1-Ubc9 was kindly provided by Dr Van G. Wilson (Texas A&M University System Health Science Center, Dallas, TX). Histone deacetylase 7 (HDAC7) was amplified using a pair of primers, CCACCATGCACAGCCCCGGCGCTGAT and CCTTAGAGATTCATAGGTTCTTCCTCCT, and cloned into pcDNA3.1. A plasmid encoding His-tagged mature SUMO1 (His-SUMO1) was reconstructed from pcDNA3.1-SUMO1 (GG).[11] His-tagged mature SUMO2 (His-SUMO2) was amplified using a pair of primers, CCACCATGCACCATCATCACCACCATGAGACTCCGGCGCTCGCCATGG and TCAACCTCCCGTCTGCTGTTGGAACACATCA, and subcloned into pcDNA3.1. The serially truncated forms of β-catenin cDNA were subcloned into pBIND (Promega). Glutathione *S*-transferase (GST)-PML-IV was constructed by subcloning PML-IV cDNA into pEU-E01-MCS (CellFree Science, Matsuyama, Japan). SUMOylation site-mutated PML-IV was constructed by mutagenesis of GST-PML-IV or Flag-PML-IV using the following primers: K65R-F, CGGTGCCCGAAGCTGCTGCCTTGT; K65R-R, GGCTTCCGCCTGGCATTGCT; K160R-F, CGGCACGAGGCCCGGCCCCTAGCAGA; K160R-R, GAGGAACCACTGGTGTGCCTCGAAGCA; K490R-F, CGGATGGAGTCTGAGGAGGGGAAGGAGGCAA; and K490R-R, GATGACCTTCCTGGGGCACTGGGT. Reporter plasmids encoding p53-responsive firefly luciferase as well as constitutively expressing Renilla luciferase were purchased from SA Biosciences (Frederick, MD).

Silencer negative controls #1 and #2 and silencer small interfering RNA (siRNA) for *CTNNB1* (#42816 and #3000; Ambion, Austin, TX) were used at a final concentration of 20 nmol/L. siRNAs for RanBP2 have been described previously.[11] Transient transfections were performed using the Lipofectamine 2000 and Plus reagents (Invitrogen, Carlsbad, CA) in accordance with the manufacturer's protocol. The total amount of DNA was adjusted by adding relevant empty vectors.

Immunoprecipitation

Cells were lysed in immunoprecipitation buffer (250 mmol/L NaCl, 50 mmol/L Tris-HCl at pH 7.5, 1 mmol/L EDTA, and 0.5% Nonidet P-40 [Fluka, Buchs, Schwitzerland]) supplemented with 1 mmol/L NaF, 10 mmol/L *N*-ethylmaleimide (Sigma-Aldrich), a phosphatase inhibitor cocktail (Sigma-Aldrich), and a protease inhibitor cocktail (Roche, Mannheim, Germany). The lysate was incubated with anti-Flag M2 monoclonal antibody (Sigma-Aldrich), anti-β-catenin monoclonal antibody (clone 14; BD Transduction Laboratories, Palo Alto, CA), anti-TCF4 monoclonal antibody (6H5-3; Upstate, Charlottesville, VA), anti-polyhistidine (clone HIS-1; Sigma-Aldrich), or relevant control immunoglobulin G at 4°C overnight and precipitated with Dynabeads protein G (Dynal Biotech, Oslo, Norway). Immunoprecipitates were washed 5 times with the ice-cold immunoprecipitation buffer and resolved by sodium dodecyl sulfate-polyacrylamide gel electrophoresis (SDS-PAGE).

Immunoblotting

Protein samples were fractionated by SDS-PAGE and blotted onto Immobilon-P membranes (Millipore, Billerica, MA). After incubation with primary antibodies at 4°C overnight, the blots were detected with relevant horseradish peroxidase-conjugated anti-mouse or anti-rabbit immunoglobulin G antibody and ECL Western Blotting Detection Reagents (GE Healthcare, Chalfont St. Giles, United Kingdom). Blot intensity was quantified using a LAS-3000 scanner and Science Lab 2003 software (Fuji Film, Tokyo, Japan).

Anti-β-catenin (clone 14, BD Transduction Laboratories), anti-β-catenin (Cell Signaling Technology, Beverly, MA), anti-TCF4 (6H5-3; Upstate), anti-TCF4 (Santa Cruz Biotechnology, Santa Cruz, CA), anti-GAL4 (RK5C1; Santa Cruz Biotechnology), anti-polyhistidine (clone HIS-1; Sigma-Aldrich), anti-SUMO1 (Biomol Research Laboratory, Plymouth Meeting, PA), anti-SUMO2/3 (Biomol Research Laboratory), anti-β-actin (AC-74; Sigma-Aldrich), anti-p53 (DO-1; Santa Cruz Biotechnology), anti-PML (H-238; Santa Cruz Biotechnology), anti-Ubc9 (Abgent, San Diego, CA), and anti-HDAC7 (XX-7; Santa Cruz Biotechnology) antibodies as well as peroxidase-conjugated anti-Flag (M2; Sigma-Aldrich) antibody were used as the primary antibodies.

Immunofluorescence Microscopy

Cells cultured on glass coverslips (Asahi Technoglass, Tokyo, Japan) were fixed with 4% formaldehyde at room temperature for 10 minutes, permeabilized with 0.1% Triton X-100, and blocked with 10% normal swine serum (Vector Laboratories, Burlingame, CA). Twelve specimens of sporadic colorectal cancer were selected from the pathology archive panel of the National Cancer Center Hospital (Tokyo, Japan). The specimens were incubated with primary antibodies at 4°C overnight and subsequently with Alexa Fluor-conjugated secondary antibodies (Invitrogen). Images were taken on a Zeiss Axioplan 2 microscope (Carl Zeiss, Gottingen, Germany). Primary antibodies used in this study were anti-Flag (M2), anti-HA (Bethyl Laboratories, Montgomery, TX), anti-PML-IV[29] (kindly provided by Dr Hugues de Thé and Dr Morgane Le Bras, INSERM/Centre National de la Recherche Scientifique [CNRS], Paris, France), and anti-β-catenin (clone 14) monoclonal antibodies. The protocol was reviewed and approved by the institutional ethics board of the National Cancer Center (Tokyo, Japan).

In Vitro Binding Assay

GST-fused PML-IV and the SUMOylation site-mutated recombinant proteins were synthesized using the ENDEXT Wheatgerm Expression Kit (CellFree Sciences, Matsuyama, Japan), incubated with Glutathione Sepharose 4B (GE Healthcare), washed with phosphate-buffered saline, and then eluted by adding elution buffer (50 mmol/L Tris-HCl, 10 mmol/L reduced glutathione, pH 8.0). Recombinant GST and GST-β-catenin fusion proteins were purchased from Abcam (Cambridge, England). Recombinant GST-RanBP2ΔFG (amino acids 2553–2838)[11] and His-HDAC7 proteins were purchased from Biomol Research Laboratory and Millipore, respectively.

Flag-tagged PML-IV protein was purified with anti-Flag M2 affinity gel (Sigma-Aldrich), incubated with 1 μg of GST-RanBP2ΔFG or His-HDAC7 and 1 μg of GST or GST-β-catenin, washed 5 times with phosphate-buffered saline, and then resolved by SDS-PAGE.

In Vitro SUMOylation Assay

In vitro SUMOylation was performed in a total volume of 40 μL in 40 mmol/L Tris-HCl (pH 7.5) with 0.75 mmol/L dithiothreitol at 37°C for 10 minutes (SUMO1) or 1 hour (SUMO2), terminated by addition of SDS sample buffer, and analyzed by SDS-PAGE and immunoblotting.

Results

Interaction of PML-IV With β-Catenin and TCF4

Using a comprehensive shotgun mass spectrometry approach, we had previously identified PML as 1 of 70 proteins commonly coimmunoprecipitated with anti-TCF4 antibody from 2 colorectal cancer cell lines, DLD-1 and HCT116,[11] although its biological significance had remained unexplored. The *PML* gene generates several alternatively spliced transcripts with different C-termini. Each PML isoform has different protein partners and mediates distinct cellular functions.[30] To verify the protein interaction identified by mass spectrometry and determine which PML isoform forms a complex with TCF4 and β-catenin, FLAG-tagged PML isoforms (I to V) were cotransfected with TCF4 and β-cateninΔN134 into HEK293 cells. Cell lysates were immunoprecipitated with anti-FLAG, anti-TCF4, or anti-β-catenin antibody and blotted with anti-FLAG, anti-β-catenin (β-cat), and anti-TCF4 antibodies (Figure 1*A*). We found that only PML-IV was coimmunoprecipitated with TCF4 and β-catenin, whereas the other isoforms showed no or little interaction with them. These results indicated that PML-IV is the PML isoform that interacts specifically with the TCF4 and β-catenin protein complex. We examined serial deletion mutants of β-catenin (Figure 1*B*) for binding with GST-PML-IV and found that a region containing armadillo repeats was responsible for the interaction with PML-IV (Figure 1*C*).

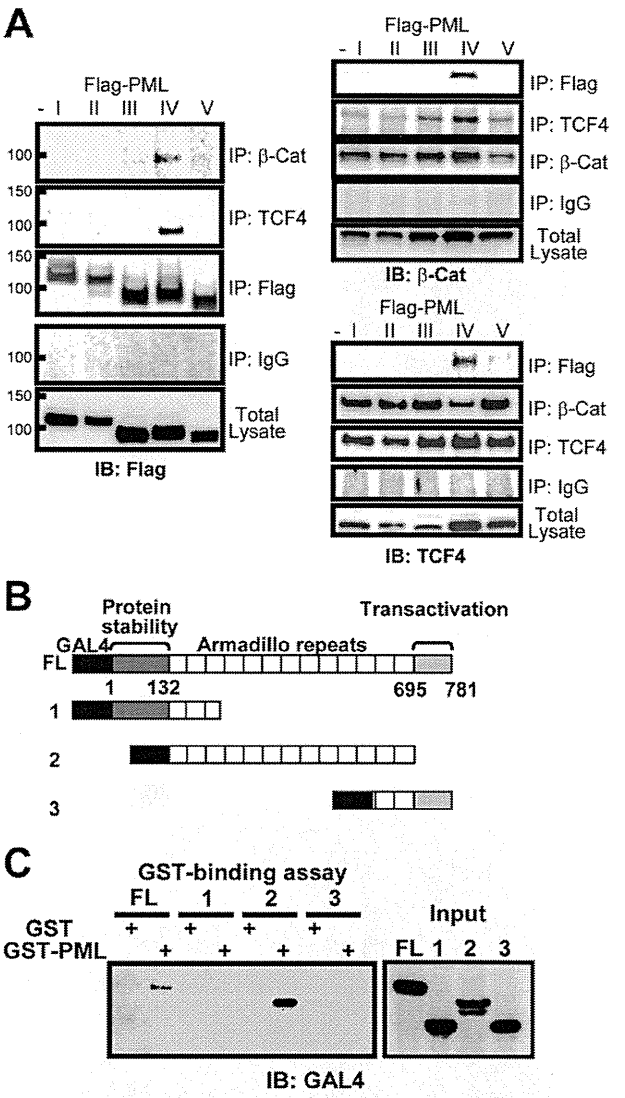

Figure 1. Interaction of PML-IV with β-catenin. (*A*) HEK293 cells were transfected with Flag-PML-I to -V, HA-β-cateninΔN134, and TCF4. The cell lysate was immunoprecipitated with anti-Flag, anti–β-catenin (β-cat), or anti-TCF4 antibody or normal mouse immunoglobulin (Ig) G. Total lysates and immunoprecipitates (IP) were immunoblotted (IB) with the indicated antibodies. (*B*) Schematic representation of the full-length (FL) and serially truncated forms of β-catenin constructs. (*C*) The β-catenin constructs were transfected into HEK293 cells. Cell lysates were incubated with GST (negative control) or GST-PML-IV, precipitated with Glutathione Sepharose 4B, and then resolved by SDS-PAGE. Total lysates (Input) and immunoprecipitates were immunoblotted with anti-GAL4 antibody.

β-Catenin Inhibits NB Formation of PML-IV

To investigate the effect of β-catenin on PML-NB formation, HeLa cells, which carry the wild-type *APC* and *CTNNB1* genes, were transfected with the Flag-tagged PML-IV (Flag-PML-IV) and HA-tagged β-cateninΔN134 constructs, and the subcellular localization of their expressed protein was examined by immunofluorescence microscopy. In HeLa cells expressing a low amount of β-catenin protein, the fine speckles of PML-IV protein were distributed uniformly within nuclei and showed the typical punctate pattern, whereas in cells expressing a high amount of β-catenin (indicated by *arrows* in Figure 2*A*) PML-IV was coarsely aggregated and distributed irregularly. These findings indicated that the presence of excess

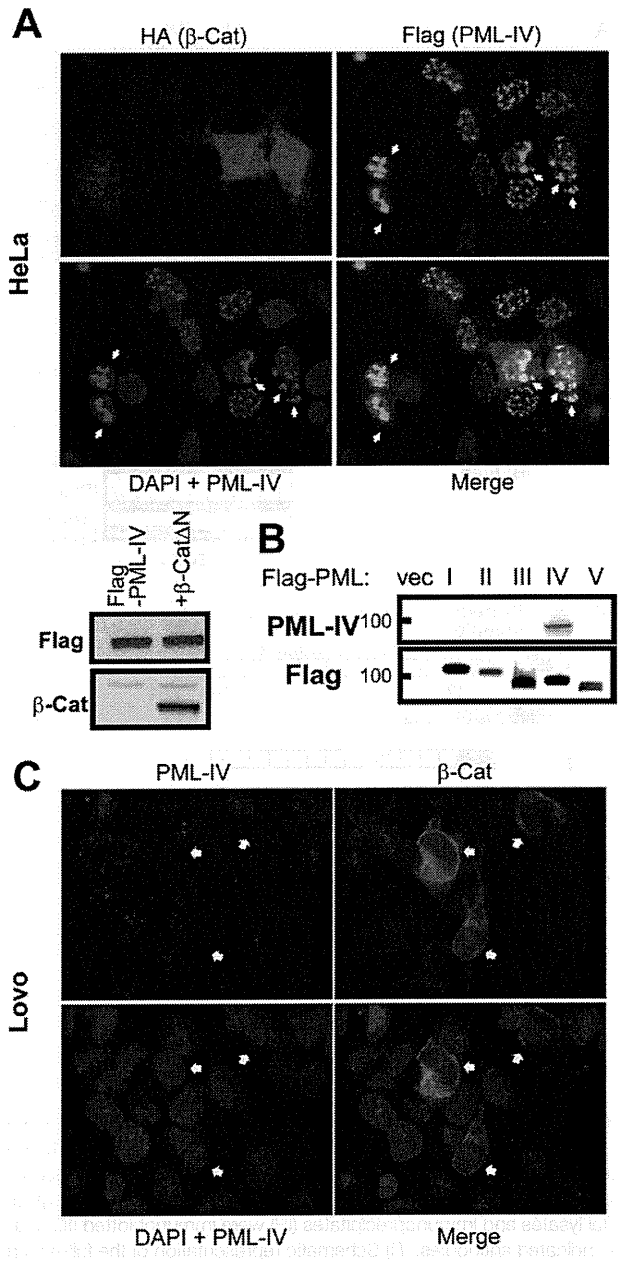

Figure 2. β-Catenin disrupts the compartmentalization of PML-IV. (*A*) HeLa cells were cotransfected with HA-β-cateninΔN134 and Flag-PML-IV and stained with anti-HA (*red*) and Flag (*green*) antibodies. Cell nuclei were visualized using 4′,6-diamidino-2-phenylindole (DAPI) (*blue*). *White arrows* indicate cells with overexpression of β-catenin and abnormal compartmentalization of PML-IV. (*B*) Control pLNCX vector (vec) or Flag-PML-I to -V was transfected into HeLa cells, and the cell lysates were immunoblotted with anti–PML-IV or anti-Flag antibody. (*C*) Lovo cells were transfected with siRNA against β-catenin. Immunofluorescence staining was performed with anti–PML-IV (*red*) and anti–β-catenin (*green*) antibodies. Cell nuclei are visualized using DAPI (*blue*).

β-catenin protein interfered with the normal compartmentalization of PML-IV.

We next examined the effect of β-catenin knockdown on PML-NB formation. Colorectal cancer cells were transfected with siRNAs against β-catenin, and the distribution of endogenous PML-IV was evaluated by immunofluorescence microscopy with isoform-specific anti–PML-IV antibody,[29] the specificity of which was confirmed by immunoblotting (Figure 2*B*). PML-IV speckles were restored by knocking down β-catenin, whereas little or broad PML-IV staining was observed in colorectal cancer cells maintaining β-catenin expression (Figure 2*C*).

In the clinical specimens from patients with colorectal cancer, normal intestinal epithelial cells without nuclear β-catenin accumulation showed the regular nuclear speckles of PML-IV, whereas no or few speckles were observed in colorectal cancer cells with nuclear β-catenin accumulation (Figure 3). These results were consistent with those of the aforementioned transfection experiments.

β-Catenin Inhibits SUMOylation of PML-IV

SUMOylation of PML is essential for the proper assembly of PML-NB. In fact, SUMOylation-deficient PML shows aberrant nuclear localization.[31,32] To test whether the aberrant PML-IV compartmentalization induced by β-catenin is due to deficient SUMOylation of PML-IV, HeLa cells were transfected with HA-β-cateninΔN134 along with Flag-tagged PML-IV and His-tagged SUMO1 (Figure 4*A*, *left*) or SUMO2 (Figure 4*A*, *right*). Immunoprecipitation and immunoblot analysis showed significantly reduced SUMOylation of PML-IV in cells cotransfected with HA-β-cateninΔN134 (Figure 4*A*). However, β-catenin did not affect the SUMOylation of PML-I or PML-III (Figure 4*B*), suggesting that the overexpression of β-catenin specifically inhibits the SUMOylation of PML-IV.

Knockdown of β-catenin in colorectal cancer DLD1 cells by siRNA (si-βc1 and si-βc2) increased the amount of PML-IV protein modified by SUMO1 (Figure 5*A*) and SUMO2 (Figure 5*B*). Similar results were obtained in 2 other colorectal cancer cell lines, Lovo and SW48 (data not shown). These data support the notion that accumulation of β-catenin interferes with the SUMOylation of PML-IV.

β-Catenin Inhibits RanBP2-Mediated SUMOylation of PML-IV

Small ubiquitin-like modifier (SUMO) proteins, a superfamily of ubiquitin-like proteins, are covalently conjugated to their substrate proteins through a cascade mediated by SUMO E1-activating, E2-conjugating, and E3-ligating enzymes. Because β-catenin did not affect the SUMOylation of PML-IV in the presence of SUMO-activating enzyme Aos1/Uba2 (E1) and conjugating enzyme Ubc9 (E2) (Figure 5*C* and *D*), we tested the effects of β-catenin on the E3-ligating reaction of PML-IV.

HDAC7[33] and RanBP2[34,35] have been shown to have the E3 SUMO ligase activity for PML and to be essential for PML-NB formation. The in vitro binding assay showed that β-catenin inhibited the physical interaction between PML-IV and RanBP2 but not that between PML-IV and HDAC7 (Figure 6*A*). We had previously identified RanBP2 as a component of the TCF4 and β-catenin complex.[11] The SUMOylation of PML-IV by RanBP2 was inhibited in the presence of β-catenin (Figure 6*B*). When RanBP2 was

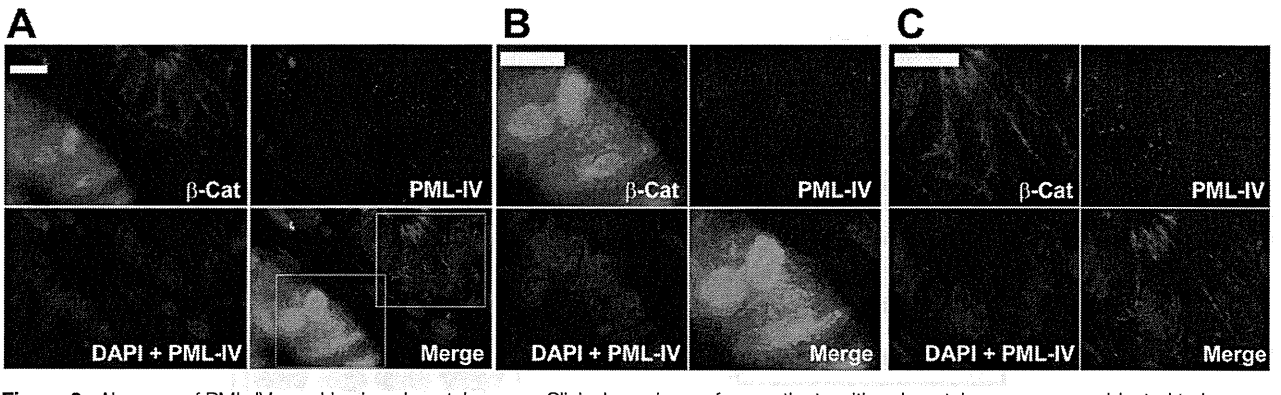

Figure 3. Absence of PML-IV speckles in colorectal cancer. Clinical specimens from patients with colorectal cancer were subjected to immunofluorescence staining with anti–PML-IV (*red*) and anti–β-catenin (*green*) antibodies. Cell nuclei are visualized using DAPI (*blue*). *Scale bar* = 10 μm. Boxed regions in *A* were enlarged and are shown in *B* and *C*.

transfected into HeLa cells, the SUMOylation of PML-IV was increased, and this increase was suppressed by coexpression of β-cateninΔN134 (Figure 6*C*). These results revealed that β-catenin prevents RanBP2-mediated enhancement of PML-IV SUMOylation by sequestering PML-IV from RanBP2.

SUMOylation of the Lysine 490 Residue of PML-IV by RanBP2

PML has several potential SUMOylation sites, each of which is considered to mediate a different aspect of the compartmentalization and stabilization of PML.[36,37] To determine the SUMOylation site of PML-IV by RanBP2, we produced PML-IV constructs mutated at the 65 (K65R), 160 (K160R), and 490 (K490R) lysine residues and assessed their SUMOylation by RanBP2 (Figure 6*D*). We found that the K65R and K160R constructs were SUMOylated by RanBP2, whereas the K490R construct was not, indicating that the lysine 490 residue of PML-IV is SUMOylated by RanBP2. To examine whether the SUMOylation at lysine 490 is essential for the proper assembly of PML-NB, HeLa cells were transfected with the Flag-PML-IV K490R, and its subcellular localization was examined by immunofluorescence microscopy.

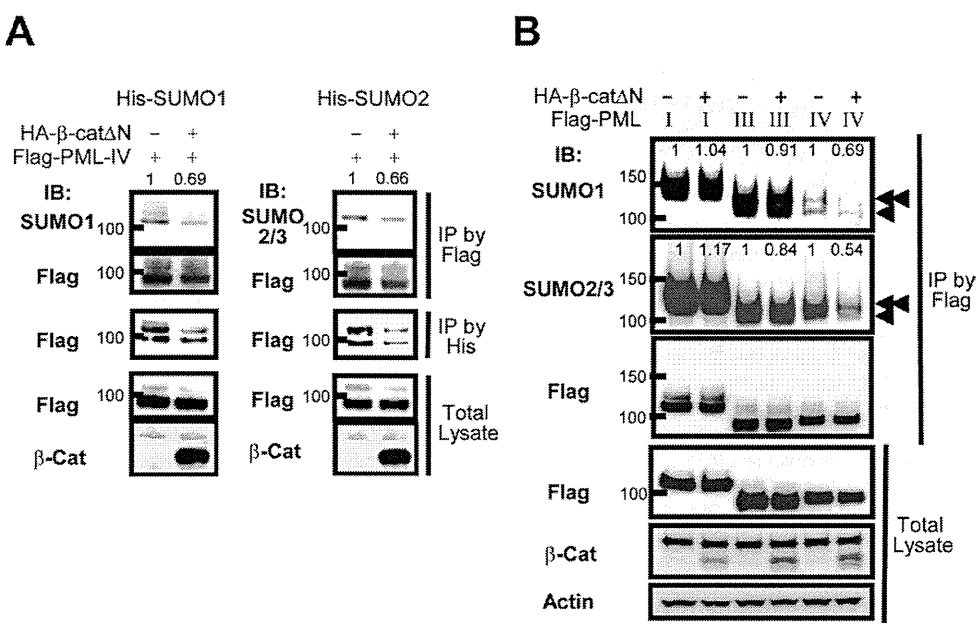

Figure 4. β-Catenin inhibits the SUMOylation of PML-IV. (*A*) Flag-PML-IV, HA-β-cateninΔN134 (HA-β-catΔN) (+) or pCIneo-HA (−), and His-SUMO1 (*left*) or His-SUMO2 (*right*) were transfected into HeLa cells as indicated. Total cell lysates were immunoprecipitated with anti-Flag or anti-His antibody. Total lysates and immunoprecipitates (IP) were immunoblotted (IB) with the indicated antibodies. Values above the blots indicate the relative amounts of SUMOylated Flag-PML-IV (SUMO1 or SUMO2/3) (normalized to immunoprecipitated Flag-PML-IV [Flag]). The values for HA-β-catΔN (−) were set at 1. (*B*) Flag-PML-I, -III, or -IV, HA-β-cateninΔN134 (HA-β-catΔN) (+) or pCIneo-HA (−), and His-SUMO1 were transfected into HeLa cells in the indicated combinations. Immunoprecipitation and immunoblotting were performed with the indicated antibodies. *Arrowheads* indicate mono-SUMOylated (*single arrowheads*) and poly-SUMOylated (*double arrowheads*) PLM-IV. Values above the blots indicate the relative amounts of SUMOylated Flag-PML-IV (SUMO1 or SUMO2/3) (normalized to immunoprecipitated Flag-PML-IV [Flag]). The values for HA-β-catΔN (−) were set at 1.

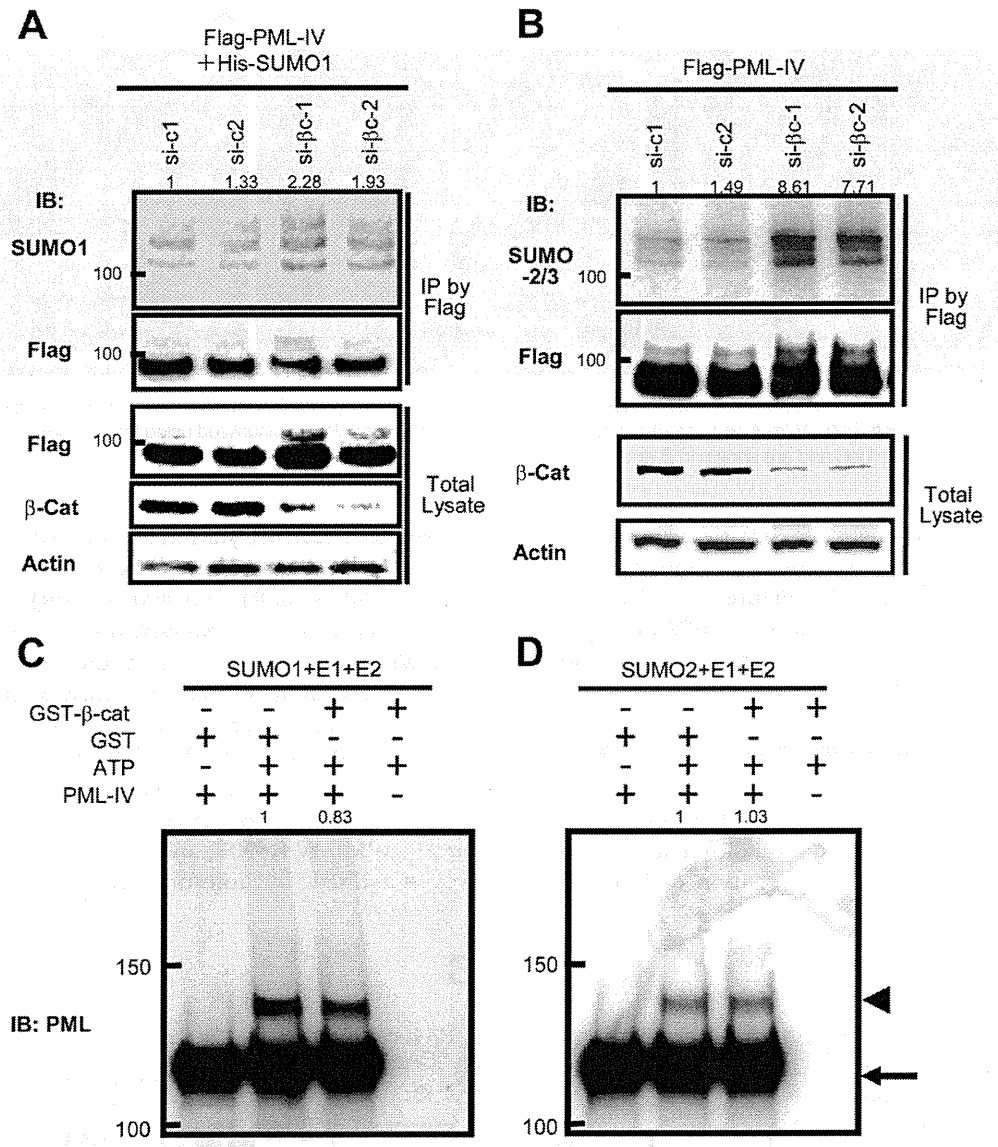

Figure 5. Knockdown of β-catenin restores the SUMOylation of PML-IV. (*A*) Flag-PML-IV, His-SUMO1, and control RNA (si-c1 or si-c2) or siRNA against β-catenin (si-βc1 or si-βc2) were transfected into DLD1 cells, and the cell lysates were immunoprecipitated with anti-Flag antibody. Total lysates and immunoprecipitates (IP) were immunoblotted (IB) with the indicated antibodies. Values above the blots indicate the amounts of SUMOylated Flag-PML-IV (SUMO1) relative to si-c1 (control siRNA) (normalized to immunoprecipitated Flag-PML-IV [Flag]). (*B*) Flag-PML-IV and control RNA (si-c1 or si-c2) or siRNA against β-catenin (si-βc1 or si-βc2) were transfected into DLD-1 cells, and the cell lysate was immunoprecipitated with anti-Flag antibody. Total lysates and immunoprecipitates were immunoblotted with the indicated antibodies. Values above the blots indicate the amounts of SUMOylated Flag-PML-IV (SUMO2/3) relative to si-c1 (control siRNA) (normalized to immunoprecipitated Flag-PML-IV [Flag]). (*C* and *D*) Purified Flag-PML-IV protein was incubated with GST (1 μg) or GST–β-catenin (β-cat) (1 μg), SUMO-activating enzyme Aos1/Uba2 (E1) (0.3 μg), conjugating enzyme Ubc9 (E2) (0.2 μg), and (*C*) His-SUMO1 (3 μg) or (*D*) His-SUMO2 (3 μg) at 37°C for 1 hour in the presence or absence of 4 mmol/L adenosine triphosphate (ATP), and SUMOylated PML-IV proteins were detected as slowly migrating bands (indicated by an *arrowhead*) by immunoblotting with anti-PML antibody. Values above the blots indicate the relative amounts of SUMOylated Flag-PML-IV (*arrowhead*) (normalized to immunoprecipitated Flag-PML-IV [*arrow*]).

PML-IV K490R was coarsely aggregated and distributed irregularly (Figure 6*E*).

β-Catenin Abrogates the Transactivation of TP53 by PML-IV

Finally we examined whether the abrogation of PML-IV compartmentalization by β-catenin leads to the suppression of PML function. p53 activity is regulated by PML, and stabilization of the p53 protein mediates in part the tumor-suppressor function of PML.[38–40] Consistently, the luciferase activity driven by the p53-responsive promoter was enhanced 2-fold by transfection with PML-IV, and the enhancement was suppressed by increasing the amount of coexpressed β-catenin (Figure 7*A*). Overexpression of PML-IV induced the accumulation of p53 protein, and this was suppressed by increasing the amount of

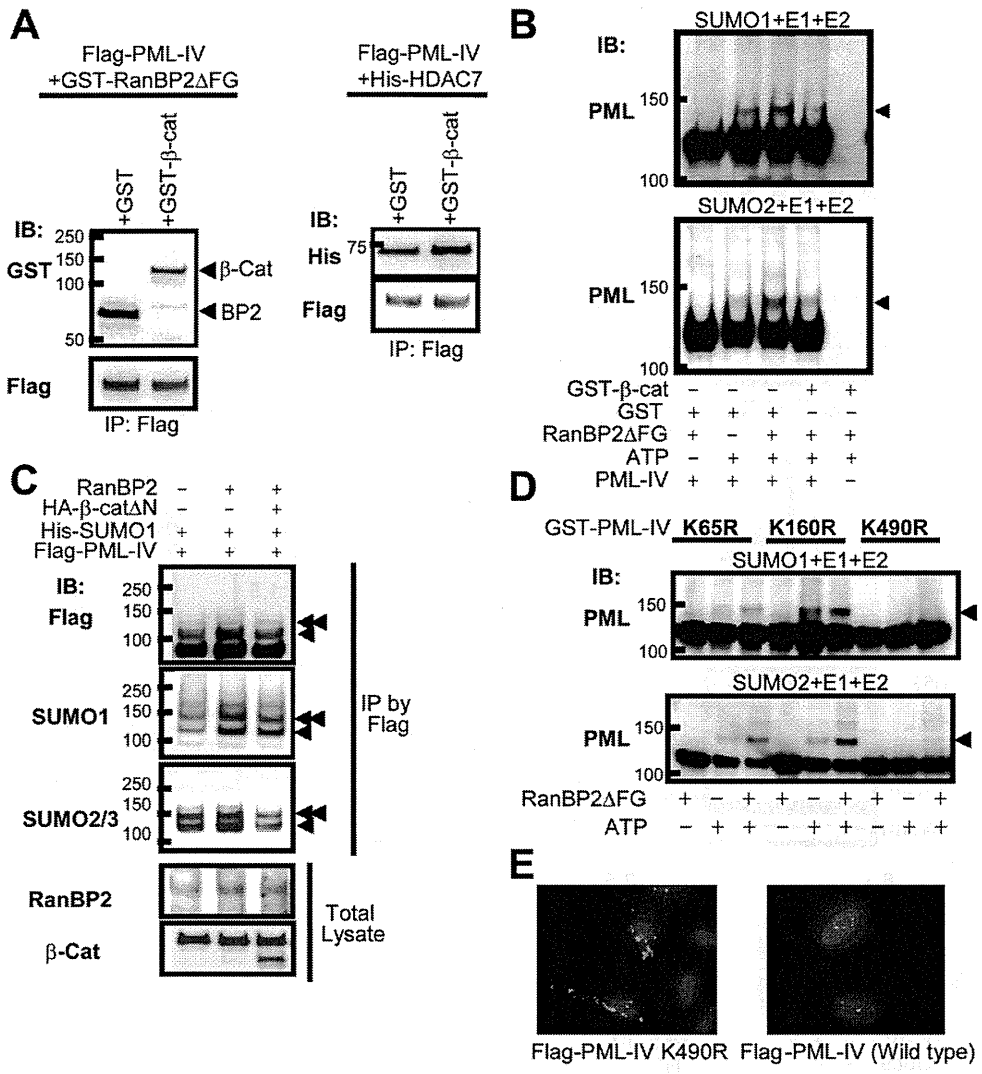

Figure 6. β-Catenin inhibits RanBP2-mediated SUMOylation of PML-IV. (*A*) Purified Flag-PML-IV protein and GST-RanBP2ΔFG or His-HDAC7 were incubated in the presence of GST or GST-β-catenin protein, immunoprecipitated (IP) with anti-Flag antibody, and immunoblotted (IB) with anti-GST, anti-His, or anti-Flag antibody. (*B*) Recombinant PML-IV, RanBP2dFG (25 ng), and GST or GST-β-catenin (1 μg) were incubated with E1 (0.3 μg), E2 (0.2 μg), SUMO1 (3 μg) or SUMO2 (3 μg), and 4 mmol/L adenosine triphosphate (ATP) as indicated. (*C*) Flag-PML-IV, His-SUMO1, HA-β-cateninΔN134 (HA-β-catΔN), and RanBP2 were transfected into HeLa cells in the indicated combinations. Immunoprecipitation and immunoblotting were performed with the indicated antibodies. (*D*) Recombinant GST-PML-IV protein with mutation in the lysine 65, 160, or 490 residue and RanBP2ΔFG (25 ng) were incubated with E1 (0.3 μg), E2 (0.2 μg), SUMO1 (3 μg) or SUMO2 (3 μg), and 4 mmol/L ATP as indicated. SUMOylated PML-IV (indicated by *arrowheads*) was detected by SDS-PAGE and immunoblotting with anti-PML antibody. (*E*) HeLa cells were transfected with Flag-PML-IV K490R (*left*) or with Flag-PML-IV (wild type) and stained with anti-Flag (*green*) antibody. Nuclei were visualized with DAPI staining (*blue*).

coexpressed β-catenin (Figure 7*B*). Furthermore, p53 accumulation by PML-IV was enhanced by RanBP2, and the enhancement was abrogated by the coexpression of β-catenin (Figure 7*C*). Knockdown of RanBP2 suppressed p53-responsive promoter activity (Figure 7*D*), and the PML mutants K490R and K160R failed to fully activate the p53-responsive promoter (Figure 7*E*). SUMOylation of the lysine 160 residue of PML-IV by SUMO3 has also been shown to be essential for PML-NB formation.[41] Enhancement of p53-responsive promoter activity by Ubc9 or HDAC7 was insensitive to β-catenin (Figure 7*F*). All these results indicate that the lysine 490 residue of PML-IV is the likely RanBP2 target site and that β-catenin inhibits the SUMOylation via competitive binding with RanBP2.

Discussion

Aberrant activation of Wnt signaling and subsequent accumulation of β-catenin has been considered a major force driving development of colorectal cancer, but β-catenin is a multifunctional protein, and the entire process of carcinogenesis mediated by its accumulation has not been fully explained. In this study, we revealed a

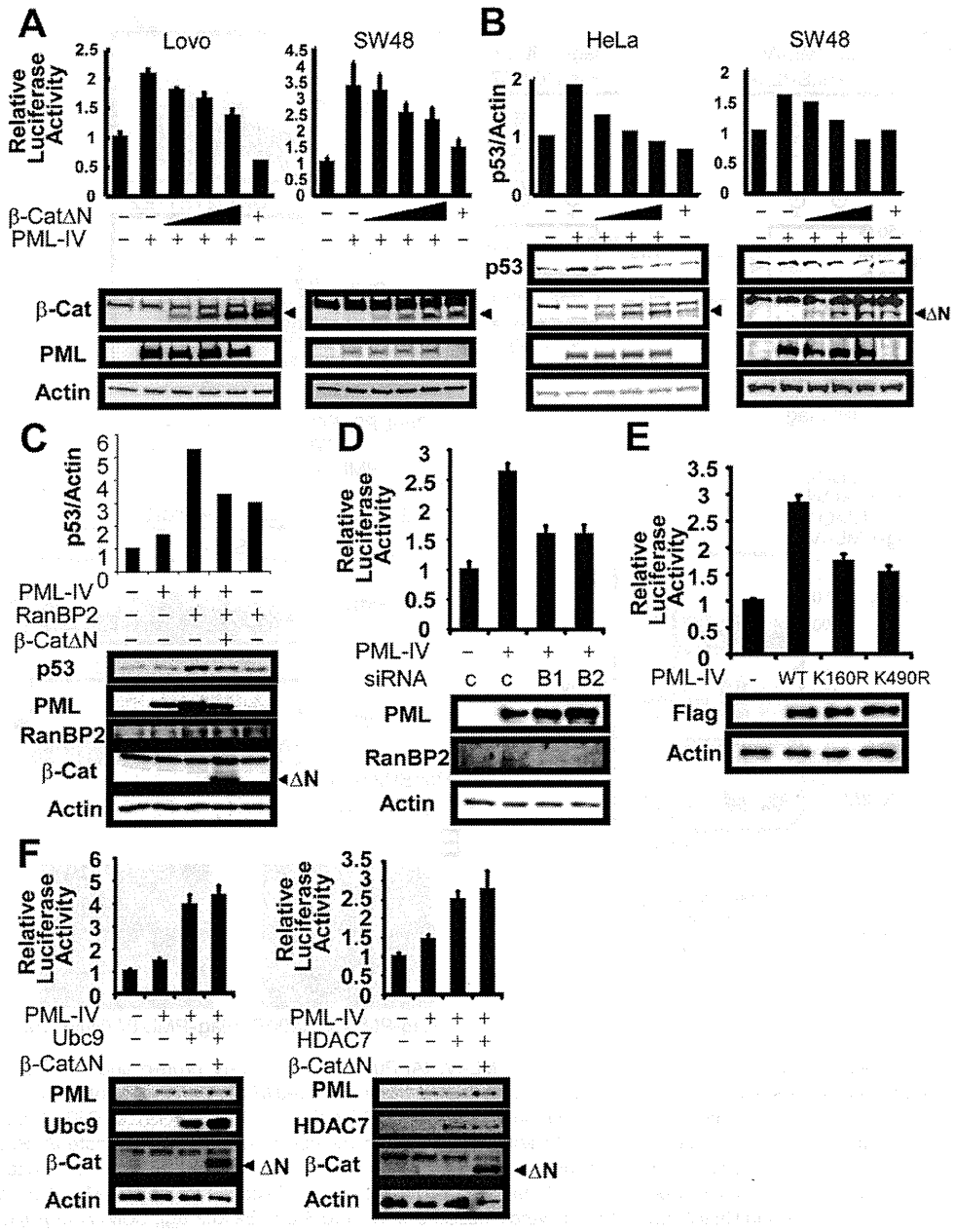

Figure 7. β-Catenin interferes with p53 activation by PML-IV. (*A*) Lovo or SW48 cells were transfected in triplicate with a p53-responsive firefly luciferase construct, a constitutively expressed Renilla luciferase construct, Flag-PML-IV, and β-cateninΔN134 (β-catΔN) or their relevant empty vectors as indicated. Forty-eight hours after transfection, luciferase activity was measured using Renilla luciferase activity as the internal control. *Bars* represent SD. (*B*) Flag-PML-IV and β-cateninΔN134 (β-catΔN) were transfected into HeLa or SW48 cells as indicated. Twenty-four hours later, the cells were treated with mitomycin C (10 μmol/L) for 3 hours and harvested with SDS sample buffer. Lysates were immunoblotted with the indicated antibodies. The intensity of the blots was quantified by densitometry, and the expression level of p53 protein relative to β-actin (internal control) was calculated. (*C*) Flag-PML-IV, RanBP2, and β-cateninΔN134 (β-catΔN) were transfected into HeLa cells as indicated. The relative expression level of p53 protein was determined as described in *B*. (*D*) Lovo cells were transfected in triplicate with a p53-responsive firefly luciferase construct, a Renilla luciferase construct, Flag-PML-IV, and siRNA (C, control; B1 and B2, siRNA for RanBP2[11]) as indicated. Luciferase activity was measured as described in *A*. (*E*) Lovo cells were transfected in triplicate with a p53-responsive firefly luciferase construct, a constitutively expressed Renilla luciferase construct, and Flag-PML-IV (WT, K160R, or K490R) as indicated, and luciferase activity was measured as described in *A*. (*F*) Lovo cells were transfected in triplicate with a p53-responsive firefly luciferase construct, a constitutively expressed Renilla luciferase construct, Flag-PML-IV, Ubc9, HDAC7, and β-cateninΔN134 (β-catΔN) as indicated, and luciferase activity was measured as described in *A*.

novel posttranslational mechanism by which β-catenin abrogated PML tumor suppressor function. β-catenin forms a complex specifically with PML-IV (Figure 1) and sequesters PML-IV from RanBP2 (Figure 6*A*). RanBP2 has been shown to be an E3 ligase for PML-IV,[34,35] and this sequestering inhibited the SUMOylation of PML-IV (Figure 6*B* and *C*). SUMOylation of PML is essential for the recruitment of several PML-binding proteins and

proper assembly of PML-NB.[32,37,42] The accumulation of β-catenin was closely associated with aberrant PML-NB formation in clinical samples (Figure 3). We conclude that β-catenin disrupts PML-NB formation by inhibiting the SUMOylation of PML-IV by RanBP2. However, the possibility that RanBP2 regulates other scaffold or associated proteins that aid the recruitment of PML-IV could not be fully excluded.

The integrity of PML-NB is essential for proper gene transcription. We observed that β-catenin inhibited the PML-mediated enhancement of promoter-specific transcriptional activity of p53 tumor suppressor protein (Figure 7). PML interacts with p53 protein and recruits it into PML-NB.[38] The disruption of PML-NB formation by β-catenin thus seems to inhibit the recruitment of p53 and its tumor-suppressor function.

Reduced expression of PML protein is not limited to colorectal cancer but has also been reported in various human solid tumors, including cancers of the prostate, breast, lung, and brain,[26] where this loss of expression is associated with aggressive tumor behavior in some cases. However, expression of the *PML* gene was well maintained, and its mutation was rare in solid tumors, indicating the contribution of certain posttranslational mechanisms to the reduction of PML protein expression. A recent study has shown that SUMOylation of PML leads to its degradation through recognition by the E3 ubiquitin ligase RNF4/SNURF, a protein containing 4 SUMO interaction motifs.[43] On the other hand, it has also been shown that SUMOylation inhibits the degradation of PML by Pin1, peptidyl-prolyl cis-trans isomerase, which binds to phosphorylated PML and promotes a conformational change triggering its degradation.[44] This apparent contradiction could be explained by assuming that each SUMOylation site in PML mediates a different function.[36] SUMOylation of the lysine 160 residue promotes PML degradation by RNF4/SNURF, whereas SUMOylation of lysine 490 inhibits PML degradation.[43] RanBP2 SUMOylates the lysine 490 residue, but not the lysine 160 residue, of PML-IV (Figure 6*D*). β-Catenin is considered to promote the dysfunction of PML through inhibition of residue-specific SUMOylation.

The Wnt signaling pathway plays important roles in the maintenance of intestinal epithelial stem cell reservoirs.[45] Constitutive activation of the pathway has been implicated in the maintenance of the undifferentiated status and self-renewal of colorectal cancer cells. Recently, PML was also reported to be essential for the maintenance of hematopoietic stem and quiescent leukemia-initiating cells.[46] The inorganic arsenite arsenic trioxide has been shown to target PML for degradation[47] and to eradicate quiescent leukemia-initiating chronic myeloid leukemia cells.[46] In the present study, although we focused mainly on the inhibition of PML SUMOylation by β-catenin, the interaction between the 2 proteins may have different functional aspects that are essential for the regulation of stem cell phenotype. It will be necessary to further clarify the entire signaling pathway mediated by these proteins.

References

1. Kinzler KW, Vogelstein B. Lessons from hereditary colorectal cancer. Cell 1996;87:159–170.
2. Morin PJ, Sparks AB, Korinek V, et al. Activation of beta-catenin-Tcf signaling in colon cancer by mutations in beta-catenin or APC. Science 1997;275:1787–1790.
3. Sparks AB, Morin PJ, Vogelstein B, et al. Mutational analysis of the APC/beta-catenin/Tcf pathway in colorectal cancer. Cancer Res 1998;58:1130–1134.
4. Barker N, Morin PJ, Clevers H. The yin-yang of TCF/beta-catenin signaling. Adv Cancer Res 2000;77:1–24.
5. Shitashige M, Hirohashi S, Yamada T. Wnt signaling inside the nucleus. Cancer Sci 2008;99:631–637.
6. Idogawa M, Yamada T, Honda K, et al. Poly(ADP-ribose) polymerase-1 is a component of the oncogenic T-cell factor-4/beta-catenin complex. Gastroenterology 2005;128:1919–1936.
7. Idogawa M, Masutani M, Shitashige M, et al. Ku70 and poly(ADP-ribose) polymerase-1 competitively regulate beta-catenin and T-cell factor-4-mediated gene transactivation: possible linkage of DNA damage recognition and Wnt signaling. Cancer Res 2007;67:911–918.
8. Sato S, Idogawa M, Honda K, et al. beta-catenin interacts with the FUS proto-oncogene product and regulates pre-mRNA splicing. Gastroenterology 2005;129:1225–1236.
9. Shitashige M, Naishiro Y, Idogawa M, et al. Involvement of splicing factor-1 in beta-catenin/T-cell factor-4-mediated gene transactivation and pre-mRNA splicing. Gastroenterology 2007;132:1039–1054.
10. Hayashida Y, Honda K, Idogawa M, et al. E-cadherin regulates the association between beta-catenin and actinin-4. Cancer Res 2005;65:8836–8845.
11. Shitashige M, Satow R, Honda K, et al. Regulation of Wnt signaling by the nuclear pore complex. Gastroenterology 2008;134:1961–1971, 1971 e1–4.
12. Kakizuka A, Miller WH Jr, Umesono K, et al. Chromosomal translocation t(15;17) in human acute promyelocytic leukemia fuses RAR alpha with a novel putative transcription factor, PML. Cell 1991;66:663–674.
13. de The H, Lavau C, Marchio A, et al. The PML-RAR alpha fusion mRNA generated by the t(15;17) translocation in acute promyelocytic leukemia encodes a functionally altered RAR. Cell 1991;66:675–684.
14. Wang ZG, Delva L, Gaboli M, et al. Role of PML in cell growth and the retinoic acid pathway. Science 1998;279:1547–1551.
15. Piazza F, Gurrieri C, Pandolfi PP. The theory of APL. Oncogene 2001;20:7216–7222.
16. Melnick A, Licht JD. Deconstructing a disease: RARalpha, its fusion partners, and their roles in the pathogenesis of acute promyelocytic leukemia. Blood 1999;93:3167–3215.
17. Salomoni P, Pandolfi PP. The role of PML in tumor suppression. Cell 2002;108:165–170.
18. Bernardi R, Papa A, Pandolfi PP. Regulation of apoptosis by PML and the PML-NBs. Oncogene 2008;27:6299–6312.
19. Salomoni P, Ferguson BJ, Wyllie AH, et al. New insights into the role of PML in tumour suppression. Cell Res 2008;18:622–640.
20. Labbaye C, Valtieri M, Grignani F, et al. Expression and role of PML gene in normal adult hematopoiesis: functional interaction between PML and Rb proteins in erythropoiesis. Oncogene 1999;18:3529–3540.
21. Guo A, Salomoni P, Luo J, et al. The function of PML in p53-dependent apoptosis. Nat Cell Biol 2000;2:730–736.
22. Bernardi R, Guernah I, Jin D, et al. PML inhibits HIF-1alpha translation and neoangiogenesis through repression of mTOR. Nature 2006;442:779–785.
23. Wang ZG, Ruggero D, Ronchetti S, et al. PML is essential for multiple apoptotic pathways. Nat Genet 1998;20:266–272.
24. Rego EM, Pandolfi PP. Analysis of the molecular genetics of acute promyelocytic leukemia in mouse models. Semin Hematol 2001;38:54–70.

JJCO Japanese Journal of Clinical Oncology

Jpn J Clin Oncol 2011;41(7)847–853
doi:10.1093/jjco/hyr060
Advance Access Publication 15 May 2011

Combined Functional Genome Survey of Therapeutic Targets for Clear Cell Carcinoma of the Kidney

Hideaki Ito[1,2], Kazufumi Honda[1], Reiko Satow[1], Eri Arai[3], Miki Shitashige[1], Masaya Ono[1], Tomohiro Sakuma[4], Shigeru Sakano[2], Katsusuke Naito[2,5], Hideyasu Matsuyama[2] and Tesshi Yamada[1,*]

[1]Divisions of Chemotherapy and Clinical Research, National Cancer Center Research Institute, Tokyo, [2]Department of Urology, Graduate School of Medicine, Yamaguchi University, Ube, [3]Divisions of Molecular Pathology, National Cancer Center Research Institute, Tokyo, [4]BioBusiness Group, Mitsui Knowledge Industry, Tokyo, and [5]Department of Urology, Mine City Hospital, Mine, Japan

*For reprints and all correspondence: Tesshi Yamada, Division of Chemotherapy and Clinical Research, National Cancer Centre Research Institute, Tokyo 104-0045, Japan. E-mail: tyamada@ncc.go.jp

Received January 6, 2011; accepted April 9, 2011

Objective: Emerging molecular targeting therapeutics have been incorporated into the management of advanced renal cell carcinoma; however, their efficacy remains limited. The aim of this study was to catalog potential therapeutic target molecules for renal cell carcinoma.
Methods: We first selected genes up-regulated in clear cell renal cell carcinoma relative to surrounding normal kidney tissues in 10 patients (Study Cohort) using high-density exon arrays that detect all potential transcripts predicted in the human genome. The selected genes were subjected to independent validation in another set of 10 patients (Validation Cohort) using real-time reverse transcriptase polymerase chain reaction and functional screening using small interfering RNA in six clear cell renal cell carcinoma cell lines.
Results: We identified 164 genes whose expression was significantly elevated in clear cell renal cell carcinoma ($P < 0.0001$ [Student's *t*-test] and at least a 3-fold change in transcription signal). We finally extracted 33 genes required for maintaining cell proliferation in at least two clear cell renal cell carcinoma cell lines. The 33 genes included 13 genes known to be associated with the development/progression of renal cell carcinoma, including *CAIX* and *FLT-1*, confirming the robustness of the current strategy.
Conclusions: Through a combination of genome-wide expression and functional assays, we identified a set of genes with high potential as targets for drug development. This method is rapid and comprehensive and could be applied to the discovery of diagnostic biomarkers and therapeutic targets for cancers other than clear cell renal cell carcinoma.

Key words: exon array – functional screening – molecular targeting therapy – renal cell carcinoma – small interfering RNA

INTRODUCTION

Renal cell carcinoma (RCC) accounts for 3–4% of all human malignancies and is the 10th leading cause of cancer-related death in men (1). A quarter of RCC patients present with locally advanced or metastatic RCC (2). Surgical resection of the affected kidney is the most reliable treatment modality for localized RCC, while a third of such patients experience recurrence. RCC is not generally sensitive to chemotherapy or radiotherapy, and although immunotherapy using interferon-α or interleukin-2 has some efficacy, the overall response rate is limited to 10–15% and the median survival period of patients with metastatic RCC remains about 13 months (2).

Clear cell carcinoma is the major histological type, accounting for ~70–80% of RCC. The majority of clear cell RCC (CCRCC) carries the somatic mutation of the von Hippel-Lindau (*VHL*) gene (3). The functional loss of the *VHL* gene induces the overexpression of the transcription factor hypoxia inducible factor 1 and its downstream target genes, vascular endothelial growth factors (*VEGF*), glucose transporter, platelet-derived growth factor (*PDGF*) and transforming growth factor-α (*TGF*-α) (4). In

addition, the activation of the mammalian target of rapamycin (mTOR) signaling pathway has also been documented in CCRCC (5). Thus, anti-VEGF antibody (bevacizumab), small-molecule multikinase inhibitors that inhibit VEGF receptors (sorafenib, sunitinib, pazopanib and axitinib) and mTOR inhibitors (everolimus and temsirolimus) were recently developed, and these have been reported to have a favorable safety profile and to prolong time to progression for advanced RCC patients (6,7). However, such novel agents never eradicate cancer cells, and offer only a limited benefit to patients in terms of survival period (6–8). These facts indicate that there is an urgent need for developing new therapeutics.

In the present study, we adopted an unbiased genomic approach to identify genes involved in the growth of CCRCC cells. Here, we report 33 potential therapeutic targets for CCRCC.

PATIENTS AND METHODS

Tissue Samples

Sufficient amounts of surgically resected tissue were obtained from 20 patients who underwent radical nephrectomy at the National Cancer Center Hospital (Tokyo, Japan) for the treatment of histopathologically confirmed CCRCC in 2005–2006 (Study Cohort, $n = 10$) and in 1999 (Validation Cohort, $n = 10$), and all patient submitted written informed consent. The clinicopathological characteristics of these 20 patients are shown in Table 1. All patients underwent chest X-ray, computed tomography scan and bone scan examinations, and were staged in accordance with the American Joint Committee on Cancer /International Union Against Cancer TNM classification, fifth edition (1997). None of the patients received any preoperative treatments. Following nephrectomy, tumor and surrounding non-tumorous kidney tissues were immediately frozen in liquid nitrogen. The protocol of this study was reviewed and approved by the ethics committee of the National Cancer Center.

RNA Extraction

Approximately 50 mg of frozen tissue was homogenized in 0.5 ml TRIzol (Invitrogen, Carlsbad, CA), and total RNA was extracted according to the protocol of the supplier. RNA

Table 1. Clinicopathological characteristics of patients with clear cell renal cell carcinoma (CCRCC) in this study

Age	Sex	Histology	Tumor size (mm)	Grade	v	pV	pT	pN	M (organ)	Stage
Study set ($n = 10$)										
51	Male	Clear cell	25	2	0	0	1a	0	0	1
66	Female	Clear cell	60	1	1	1	3b	0	0	3
55	Female	Clear cell	45	1	0	0	1b	0	0	1
56	Male	Clear cell	80	3	1	1	3b	0	0	3
77	Male	Clear cell	25	1	0	0	1a	0	0	1
63	Female	Clear cell	95	1	1	0	3a	0	0	3
78	Male	Clear cell	65	1	1	0	1b	0	0	1
53	Male	Clear cell	28	1	0	0	1a	0	0	1
55	Male	Clear cell	25	1	0	0	1a	0	0	1
64	Male	Clear cell	50	1	0	0	1b	0	0	1
Validation set ($n = 10$)										
39	Male	Clear cell	40	1	0	0	1a	0	0	1
45	Male	Clear cell	23	1	0	0	1a	0	0	1
70	Male	Clear cell	55	1	0	0	1b	0	0	1
68	Male	Clear cell	70	3	1	1	3b	0	1 (Lung)	4
42	Male	Clear cell	50	2	0	0	1b	0	0	1
56	Male	Clear cell	48	3	0	0	1b	0	1 (Bone)	4
55	Female	Clear cell	13	3	0	0	1a	0	1 (Liver/stomach)	4
62	Male	Clear cell	75	3	0	0	1b	0	0	1
49	Male	Clear cell	45	2	0	0	1b	0	0	1
62	Male	Clear cell	90	2	0	0	3a	0	0	3

v, vascular involvement; pV, renal vein tumor thrombus.

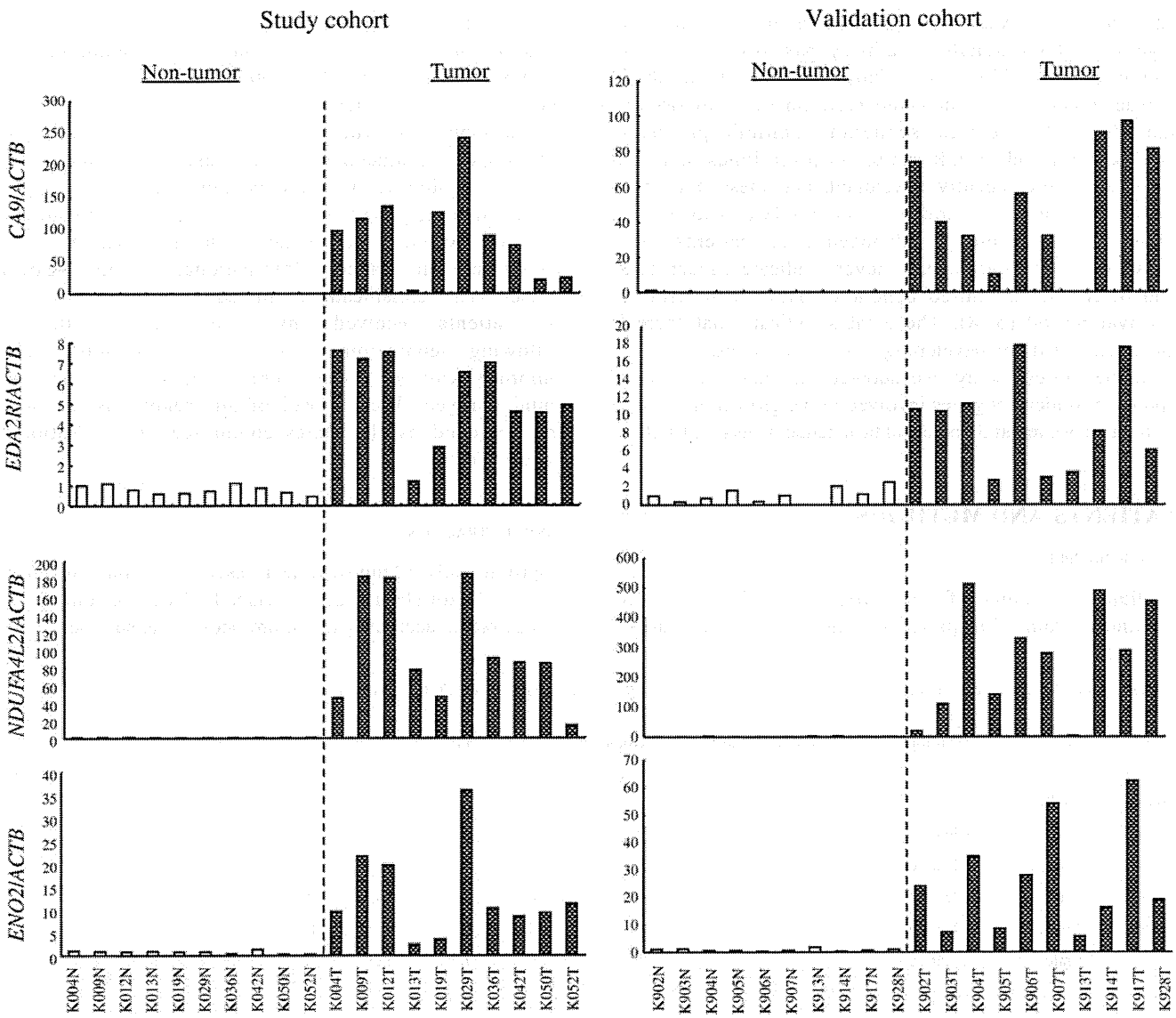

Figure 1. Real-time reverse transcription (RT) PCR analysis of *CAIX*, *EDA2R*, *NDUFA4L2* and *ENO2* genes in clear cell renal cell carcinoma (CCRCC) and surrounding renal cortex tissues.

quality was confirmed by electrophoresis, and only samples of intact RNA were used for further analysis.

RCC Cell Lines

Six human cell lines (786-O, A-498, Caki-2, VMRC-RCW, Caki-1 and OS-RC-2) derived from RCC were used in this study. 786-O, A-498 and Caki-2 were obtained from the Cell Resource Center for Biomedical Research (Sendai, Japan). VMRC-RCW and Caki-1 were from the Japan Cancer Research Cell Bank (Osaka, Japan). OS-RC-2 was from RIKEN BRC cell bank (Tokyo, Japan). Caki-1, VMRC-RCW and A-498 were maintained in Eagle's minimum essential medium (Invitrogen) supplemented with 10% fetal bovine serum. 786-O and OS-RC-2 were maintained in RPMI 1640 medium (Invitrogen) supplemented with 10% fetal bovine serum. Caki-2 was maintained in McCoy's 5A medium (Invitrogen) supplemented with 10% fetal bovine serum.

Exon Array Analysis

Total RNA (1 μg) was converted to end-labeled cRNA using a Whole Transcript Sense Target Labeling kit (Affymetrix, Santa Clara, CA) (9). Fluorescent cRNA probes were hybridized using Human Exon 1.0 ST arrays (Affymetrix), as instructed by the supplier (10). Data analysis for gene expression was carried out using the ArrayAssist software package (Version 5.5.1, Stratagene, La Jolla, CA). Antigenomic probes were used for background correction, and fluorescence intensity was normalized using the

Table 2. Biological process enrichment analysis

	All genes	Selected genes	False discovery rate
Up-regulated			
GO:0051272_positive_regulation_of_cell_motion	46	7	0.0178
GO:0051270_regulation_of_cell_motion	81	8	0.0451
GO:0030335_positive_regulation_of_cell_migration	42	6	0.0451
Down-regulated			
GO:0007588_excretion	41	13	1.08E–08
GO:0006820_anion_transport	49	11	1.74E–05
GO:0006082_organic_acid_metabolic_process	213	19	0.000359
GO:0051179_localization	1177	51	0.000553
GO:0006811_ion_transport	230	19	0.000553
GO:0019752_carboxylic_acid_metabolic_process	209	18	0.000553
GO:0043436_oxoacid_metabolic_process	209	18	0.000553
GO:0046903_secretion	168	16	0.000553
GO:0006810_transport	926	43	0.000554
GO:0042180_cellular_ketone_metabolic_process	214	18	0.000554
GO:0051234_establishment_of_localization	939	43	0.000702
GO:0015698_inorganic_anion_transport	25	6	0.00612
GO:0015711_organic_anion_transport	20	5	0.0248
GO:0006519_cellular_amino_acid_and_derivative_metabolic_process	121	11	0.0276
GO:0006835_dicarboxylic_acid_transport	5	3	0.0370

ExonRMA algorithm. Biological process enrichment analysis was performed using the GoMiner (11) with the Benjamini–Hochberg correction of the false discovery rate (FDR) for multiple tests. Only statistically significant processes showing an FDR < 0.05 were selected.

Real-time Reverse Transcription PCR

First-strand cDNA was synthesized from 1 μg of total RNA using SuperScript reverse transcriptase (Invitrogen). Real-time PCR was performed using an ABI PRISM 7000 sequence detection system (Applied Biosystems, Foster City, CA) in accordance with the manufacturer's instructions. Relative quantification was achieved by normalization against the value for the β-actin (*ACTB*) gene, as described previously (12).

Small Interfering RNA-based Functional Analysis

Three small interfering RNA (siRNA) duplexes for each of 168 genes were synthesized in a 96-well format (FlexiPlate siRNA, Qiagen, Valencia, CA) (13). The day before siRNA transfection, CCRCC cells were seeded at 2.5×10^3 cells per well in 96-well plates. Cells were then transfected with siRNA at a concentration of 10–50 nM using Lipofectamine 2000 (Invitrogen). Seventy-two hours after transfection, cell viability was quantified using CellTiter-Glo Luminescent Cell Viability Assay (Promega, Madison, WI). Luminescence was measured with a GloMax 96 Microplate Luminometer (Promega). A 10-fold serial dilution (10^{-10} to 10^{-13} M) of standard adenosine triphosphate (ATP) (Promega) was included on each assay plate in order to generate a standard curve.

RESULTS

Gene Expression Analysis

Ten paired tissue samples of CCRCC and adjacent non-tumorous kidney (Study Cohort) were subjected to genome-wide expression analysis using GeneChip Human Exon 1.0 ST Array. The array contains ~5.4 million probes grouped into 1.4 million probe sets that can interrogate over 1 million exon clusters. The design of the probes is based upon not only mRNA sequences deposited in the RefSeq and GeneBank databases, but also upon all potential exon sequences deduced within the human genome. The exon array can detect mRNAs with low abundance as well as alternatively poly-adenylated and spliced mRNA, as the probes are designed to hybridize with the entire sequences of the predicted exons.

Table 3. List of selected genes by small interfering RNA (siRNA) functional screening

Gene symbol	Gene description	Refseq ID	% Growth after siRNA transfection					
			786-O	A498	Caki-2	OS-RC-2	VMRC-RCW	Caki-1
PGF	Placental growth factor	NM_002632	82.81	60.6	87.38	98.08	112.26	75.82
PCTK3	PCTAIRE protein kinase 3	NM_002596	62.17	77.3	101.12	126.04	94.08	129.32
OLFML2A	Olfactomedin-like 2A	NM_182487	−12.42	69.8	83.27	90.59	115.21	54.15
HSF4	Heat shock transcription factor 4	NM_001040667	17.74	40.6	93.0	78.43	85.84	76.17
CP	Ceruloplasmin (ferroxidase)	NM_000096	125.97	60.2	94.55	115.97	118.55	72.89
TRIM22	Tripartite motif-containing 22	NM_006074	90.51	57.5	72.36	100.48	91.62	90.61
SNORA16A	Small nucleolar RNA, H/ACA box 16A	NR_002976	110.25	50.4	69.09	102.93	86.88	99.89
SLC2A1	Solute carrier family 2 (facilitated glucose transporter), member 1	NM_006516	78.02	76.4	95.27	91.84	102.61	98.04
SLC17A4	Solute carrier family 17 (sodium phosphate), member 4	NM_005495	77.21	−1.8	29.34	47.50	36.97	−14.40
SCARB1	Scavenger receptor class B, member 1	NM_005505	106.60	44.0	67.91	53.45	80.77	82.45
SAMD9L	Sterile alpha motif domain containing 9-like	NM_152703	70.83	78.3	101.44	82.43	92.95	88.24
RGS5	Regulator of G-protein signaling 5	NM_003617	133.09	40.2	79.82	105.81	102.54	90.52
OSMR	Oncostatin M receptor	NM_003999	80.18	78.7	108.50	94.53	117.78	105.64
NDUFA4L2	NADH dehydrogenase (ubiquinone) 1 alpha subcomplex, 4-like 2	NM_020142	60.57	68.6	99.13	90.10	103.96	89.64
MCAM	Melanoma cell adhesion molecule	NM_006500	89.80	46.8	99.13	103.91	100.23	90.65
LOXL2	Lysyl oxidase-like 2	NM_002318	128.23	51.9	75.47	109.66	105.01	73.72
ITGA5	Integrin, alpha 5 (fibronectin receptor, alpha polypeptide)	NM_002205	99.18	43.8	80.84	102.62	89.91	81.07
INHBB	Inhibin, beta B	NM_002193	110.40	39.6	74.46	105.30	77.34	100.74
IGFBP3	Insulin-like growth factor-binding protein 3	NM_001013398	91.90	42.4	95.23	74.57	93.22	96.94
FLT1	Fms-related tyrosine kinase 1 (vascular endothelial growth factor/vascular permeability factor receptor)	NM_002019	97.02	55.7	80.36	53.91	71.85	98.37
FCGR3A	Fc fragment of IgG, low affinity IIIa, receptor (CD16a)	NM_000569	116.48	58.5	91.02	67.81	89.57	101.89
FABP7	Fatty acid-binding protein 7, brain	NM_001446	127.85	54.1	74.07	106.70	107.49	90.36
EGLN3	Egl nine homolog 3 (*Caenorhabditis elegans*)	NM_022073	111.31	40.6	76.87	72.80	84.39	108.02
DIRAS2	DIRAS family, GTP-binding RAS-like 2	NM_017594	42.74	44.4	96.29	71.55	80.02	76.87
CSPG4	Chondroitin sulfate proteoglycan 4	NM_001897	70.02	79.4	107.48	84.97	94.61	113.09
CDH13	Cadherin 13, H-cadherin (heart)	NM_001257	97.73	78.8	97.71	84.94	84.69	88.69
CD200	CD200 molecule	NM_001004196	87.69	50.1	102.32	83.56	87.32	94.72
CALCRL	Calcitonin receptor-like	NM_005795	116.11	44.5	76.32	111.27	96.58	83.13
CA9	Carbonic anhydrase IX	NM_001216	7.22	10.6	14.84	60.00	48.64	−11.00
BARX2	BARX homeobox 2	NM_003658	92.70	61.0	100.83	96.22	103.86	117.49
AHNAK2	AHNAK nucleoprotein 2	NM_138420	109.69	41.3	78.06	94.93	103.92	83.69
ADM	Adrenomedullin	NM_001124	163.48	48.3	79.82	100.07	103.96	96.28
ADFP	Adipose differentiation-related protein	NM_001122	110.35	53.4	64.83	67.70	81.81	89.59

GTP, guanosine triphosphate; IgG, immunoglobulin G; NADH, nicotinamide adenine dinucleotide.

We confirmed that the transcripts of 460 annotated genes were differentially expressed between the background (non-tumorous) kidney and CCRCC tissues with statistical significance [$P < 0.0001$ (Student's t-test) and at least a 3-fold change in transcription signal]. Of the identified 460 genes, 168 transcripts were up-regulated and 292 were down-regulated in CCRCC (Supplementary data, Tables S1 and S2).

Validation of Up-regulated Genes by Real-time RT–PCR

Of the 168 up-regulated genes identified by the exon array analysis, *CAIX*, *EDA2R*, *NDUFA4L2* and *ENO2* were randomly selected for independent validation using real-time RT–PCR. The expression of these four genes was consistently elevated in 10 additional samples (Validation Cohort),

as well as in the original 10 samples (Study Cohort) of CCRCC, when compared with non-tumorous kidney tissues in the same patients, thus confirming the reproducibility of the exon array experiment (Fig. 1).

Gene Ontology Analysis

The 168 up-regulated and 292 down-regulated genes in CCRCC were subjected to gene ontology analysis (Table 2). We noted significant enrichment of genes involved in cell motion and migration among the 168 gene up-regulated in CCRCC (FDR < 0.05).

High-throughput siRNA-based Functional Screening

In order to identify genes essential for CCRCC cell proliferation and survival, six cell lines were transfected with siRNA duplexes (mixtures of three constructs per gene) targeting the 168 genes up-regulated in CCRCC on a one-gene-per-well basis. Seventy-two hours after transfection, the relative abundance of metabolically active cells was determined by quantifying the relative production of ATP. The mean ATP level in triplicate wells was normalized against those of serially diluted standard ATP and non-targeting (negative control) siRNA included on the same assay plates. We designed three siRNA constructs targeting different parts of the transcripts, and performed the transfection experiment at the lowest possible effective concentration in order to minimize off-target effects (14). We found that siRNA targeting 33 genes reduced the ATP production by more than 20% in at least two of the six RCC cell lines (Table 3).

DISCUSSION

Several new molecular targeting drugs have been approved recently for the treatment of advanced RCC, and many other compounds are under preclinical or early clinical investigation (6,7). Some of these have been shown to significantly improve quality of life, delay progression and extend survival, but rarely cure RCC patients (6,7). It is therefore necessary to identify the molecules essential for RCC cell growth and develop therapeutic approaches targeting these molecules. To date, several groups have reported the microarray-based molecular profiles of RCC (15–20); however, there have been no genome-wide functional surveys of therapeutic targets for CCRCC.

The advent of synthetic RNA interfering libraries has been reported to make systemic functional screening possible, and genes that sensitize lung cancer cells to chemotherapeutic drugs and the genes required for proliferation and survival of several cancer cell lines (13,21,22) have been successfully identified. We previously demonstrated that the combination of genome-wide expression and functional screening could be applied to the identification of therapeutic targets in hepatocellular carcinoma (9). In the present study, we screened an siRNA library targeting all 168 genes up-regulated in CCRCC, and identified 33 genes required for maintaining the viability of CCRCC cells.

Of the 33 genes, 13 [*PGF*, *SLC2A1*, *SCARB1*, *RGS5*, *IGFBP3*, *FLT-1* (*VEGFR-1*), *FABP7*, *EGLN3*, *CDH13*, *CAIX*, *ADM*, *CD200* and *ADFP*)] have previously been reported to be associated with development, progression or prognosis of RCC (23–35). This supports the suitability of our method for selecting molecular target genes. An additional 10 genes (*CP*, *OSMR*, *MCAM*, *LOXL2*, *ITGA5*, *INHBB*, *FCGR3A*, *CSPG4*, *CALCRL* and *BARX2*) have been reported to be associated with other types of cancer (14, 36–43). These genes may also be promising as molecular targets in RCC. The remaining 10 genes have not been reported to be associated with the biology of any types of cancer, and may serve as novel drug targets for CCRCC.

In the present study, we used a comprehensive genomic approach to catalog genes involved in the viability of CCRCC cells. Our method is a rapid and comprehensive approach that could be applicable to the discovery of molecular markers and therapeutic targets for CCRCC. Furthermore, our results may help us to clarify the molecular mechanisms underlying CCRCC development and progression. However, our results allow only preliminary conclusions and are limited to the listing of candidate genes. Further experimental and clinical studies of the 33 genes are necessary.

Supplementary data

Supplementary data are available at http://www.jjco.oxfordjournals.org.

Funding

This work was supported by the Third-Term Comprehensive Control Research for Cancer and Research on Biological Markers for New Drug Development conducted by the Ministry of Health and Labor of Japan, and the Program for Promotion of Fundamental Studies in Health Sciences conducted by the National Institute of Biomedical Innovation of Japan.

Conflict of interest statement

None declared.

References

1. Jemal A, Siegel R, Ward E, Hao Y, Xu J, Thun MJ. Cancer statistics, 2009. *CA Cancer J Clin* 2009;59:225–49. Epub 2009 May 27.
2. Cohen HT, McGovern FJ. Renal-cell carcinoma. *N Engl J Med* 2005;353:2477–90.
3. Kaelin WG, Jr. The von Hippel-Lindau tumor suppressor protein and clear cell renal carcinoma. *Clin Cancer Res* 2007;13:680s–4.

4. Linehan WM. Molecular targeting of VHL gene pathway in clear cell kidney cancer. *J Urol* 2003;170:593–4.
5. Robb VA, Karbowniczek M, Klein-Szanto AJ, Henske EP. Activation of the mTOR signaling pathway in renal clear cell carcinoma. *J Urol* 2007;177:346–52.
6. Costa LJ, Drabkin HA. Renal cell carcinoma: new developments in molecular biology and potential for targeted therapies. *Oncologist* 2007;12:1404–15.
7. Garcia JA, Rini BI. Recent progress in the management of advanced renal cell carcinoma. *CA Cancer J Clin* 2007;57:112–25.
8. Motzer RJ, Escudier B, Oudard S, Hutson TE, Porta C, Bracarda S, et al. Efficacy of everolimus in advanced renal cell carcinoma: a double-blind, randomised, placebo-controlled phase III trial. *Lancet* 2008;372:449–56.
9. Satow R, Shitashige M, Kanai Y, Takeshita F, Ojima H, Jigami T, et al. Combined functional genome survey of therapeutic targets for hepatocellular carcinoma. *Clin Cancer Res* 2010;16:2518–28.
10. Bemmo A, Benovoy D, Kwan T, Gaffney DJ, Jensen RV, Majewski J. Gene expression and isoform variation analysis using Affymetrix exon arrays. *BMC Genomics* 2008;9:529.
11. Zeeberg BR, Feng W, Wang G, Wang MD, Fojo AT, Sunshine M, et al. GoMiner: a resource for biological interpretation of genomic and proteomic data. *Genome Biol* 2003;4:R28.
12. Shitashige M, Naishiro Y, Idogawa M, Honda K, Ono M, Hirohashi S, et al. Involvement of splicing factor-1 in beta-catenin/T-cell factor-4-mediated gene transactivation and pre-mRNA splicing. *Gastroenterology* 2007;132:1039–54.
13. Yamaguchi U, Honda K, Satow R, Kobayashi E, Nakayama R, Ichikawa H, et al. Functional genome screen for therapeutic targets of osteosarcoma. *Cancer Sci* 2009;100:2268–74.
14. Cobellis L, Cataldi P, Reis FM, De Palo G, Raspagliesi F, Pilotti S, et al. Gonadal malignant germ cell tumors express immunoreactive inhibin/activin subunits. *Eur J Endocrinol* 2001;145:779–84.
15. Takahashi M, Rhodes DR, Furge KA, Kanayama H, Kagawa S, Haab BB, et al. Gene expression profiling of clear cell renal cell carcinoma: gene identification and prognostic classification. *Proc Natl Acad Sci USA* 2001;98:9754–9.
16. Lane BR, Li J, Zhou M, Babineau D, Faber P, Novick AC, et al. Differential expression in clear cell renal cell carcinoma identified by gene expression profiling. *J Urol* 2009;181:849–60.
17. Yao M, Tabuchi H, Nagashima Y, Baba M, Nakaigawa N, Ishiguro H, et al. Gene expression analysis of renal carcinoma: adipose differentiation-related protein as a potential diagnostic and prognostic biomarker for clear-cell renal carcinoma. *J Pathol* 2005;205:377–87.
18. Hirota E, Yan L, Tsunoda T, Ashida S, Fujime M, Shuin T, et al. Genome-wide gene expression profiles of clear cell renal cell carcinoma: identification of molecular targets for treatment of renal cell carcinoma. *Int J Oncol* 2006;29:799–827.
19. Boer JM, Huber WK, Sultmann H, Wilmer F, von Heydebreck A, Haas S, et al. Identification and classification of differentially expressed genes in renal cell carcinoma by expression profiling on a global human 31,500-element cDNA array. *Genome Res* 2001;11:1861–70.
20. Higgins JP, Shinghal R, Gill H, Reese JH, Terris M, Cohen RJ, et al. Gene expression patterns in renal cell carcinoma assessed by complementary DNA microarray. *Am J Pathol* 2003;162:925–32.
21. Whitehurst AW, Bodemann BO, Cardenas J, Ferguson D, Girard L, Peyton M, et al. Synthetic lethal screen identification of chemosensitizer loci in cancer cells. *Nature* 2007;446:815–9.
22. Schlabach MR, Luo J, Solimini NL, Hu G, Xu Q, Li MZ, et al. Cancer proliferation gene discovery through functional genomics. *Science* 2008;319:620–4.
23. Brown LF, Berse B, Jackman RW, Tognazzi K, Manseau EJ, Dvorak HF, et al. Increased expression of vascular permeability factor (vascular endothelial growth factor) and its receptors in kidney and bladder carcinomas. *Am J Pathol* 1993;143:1255–62.
24. Domoto T, Miyama Y, Suzuki H, Teratani T, Arai K, Sugiyama T, et al. Evaluation of S100A10, annexin II and B-FABP expression as markers for renal cell carcinoma. *Cancer Sci* 2007;98:77–82.
25. Fujita Y, Mimata H, Nasu N, Nomura T, Nomura Y, Nakagawa M. Involvement of adrenomedullin induced by hypoxia in angiogenesis in human renal cell carcinoma. *Int J Urol* 2002;9:285–95.
26. Furuya M, Nishiyama M, Kimura S, Suyama T, Naya Y, Ito H, et al. Expression of regulator of G protein signalling protein 5 (RGS5) in the tumour vasculature of human renal cell carcinoma. *J Pathol* 2004;203:551–8.
27. Hintz RL, Bock S, Thorsson AV, Bovens J, Powell DR, Jakse G, et al. Expression of the insulin like growth factor-binding protein 3 (IGFBP-3) gene is increased in human renal carcinomas. *J Urol* 1991;146:1160–3.
28. Krieg M, Haas R, Brauch H, Acker T, Flamme I, Plate KH. Up-regulation of hypoxia-inducible factors HIF-1alpha and HIF-2alpha under normoxic conditions in renal carcinoma cells by von Hippel-Lindau tumor suppressor gene loss of function. *Oncogene* 2000;19:5435–43.
29. Miki S, Matsumoto A, Nakamura Y, Itakura H, Kodama T, Yamamoto M, et al. Expression of scavenger receptors on renal cell carcinoma cells *in vitro*. *Biochem Biophys Res Commun* 1992;189:1323–8.
30. Morris MR, Hesson LB, Wagner KJ, Morgan NV, Astuti D, Lees RD, et al. Multigene methylation analysis of Wilms' tumour and adult renal cell carcinoma. *Oncogene* 2003;22:6794–801.
31. Tsuchiya N, Sato K, Akao T, Kakinuma H, Sasaki R, Shimoda N, et al. Quantitative analysis of gene expressions of vascular endothelial growth factor-related factors and their receptors in renal cell carcinoma. *Tohoku J Exp Med* 2001;195:101–13.
32. Yao M, Huang Y, Shioi K, Hattori K, Murakami T, Nakaigawa N, et al. Expression of adipose differentiation-related protein: a predictor of cancer-specific survival in clear cell renal carcinoma. *Clin Cancer Res* 2007;13:152–60.
33. Siva A, Xin H, Qin F, Oltean D, Bowdish KS, Kretz-Rommel A. Immune modulation by melanoma and ovarian tumor cells through expression of the immunosuppressive molecule CD200. *Cancer Immunol Immunother* 2008;57:987–96.
34. Amatschek S, Koenig U, Auer H, Steinlein P, Pacher M, Gruenfelder A, et al. Tissue-wide expression profiling using cDNA subtraction and microarrays to identify tumor-specific genes. *Cancer Res* 2004;64:844–56.
35. Bui MH, Seligson D, Han KR, Pantuck AJ, Dorey FJ, Huang Y, et al. Carbonic anhydrase IX is an independent predictor of survival in advanced renal clear cell carcinoma: implications for prognosis and therapy. *Clin Cancer Res* 2003;9:802–11.
36. Kunapuli SP, Singh H, Singh P, Kumar A. Ceruloplasmin gene expression in human cancer cells. *Life Sci* 1987;40:2225–8.
37. Lonnroth C, Andersson M, Arvidsson A, Nordgren S, Brevinge H, Lagerstedt K, et al. Preoperative treatment with a non-steroidal anti-inflammatory drug (NSAID) increases tumor tissue infiltration of seemingly activated immune cells in colorectal cancer. *Cancer Immun* 2008;8:5.
38. Peinado H, Del Carmen Iglesias-de la Cruz M, Olmeda D, Csiszar K, Fong KS, Vega S, et al. A molecular role for lysyl oxidase-like 2 enzyme in snail regulation and tumor progression. *EMBO J* 2005;24:3446–58.
39. Savarese TM, Campbell CL, McQuain C, Mitchell K, Guardiani R, Quesenberry PJ, et al. Coexpression of oncostatin M and its receptors and evidence for STAT3 activation in human ovarian carcinomas. *Cytokine* 2002;17:324–34.
40. Sellar GC, Li L, Watt KP, Nelkin BD, Rabiasz GJ, Stronach EA, et al. BARX2 induces cadherin 6 expression and is a functional suppressor of ovarian cancer progression. *Cancer Res* 2001;61:6977–81.
41. Shih IM. The role of CD146 (Mel-CAM) in biology and pathology. *J Pathol* 1999;189:4–11.
42. Yu YH, Kuo HK, Chang KW. The evolving transcriptome of head and neck squamous cell carcinoma: a systematic review. *PLoS One* 2008;3:e3215.
43. Zhang X, Green KE, Yallampalli C, Dong YL. Adrenomedullin enhances invasion by trophoblast cell lines. *Biol Reprod* 2005;73:619–26.

25. Cabrera CM, Jimenez P, Concha A, et al. Promyelocytic leukemia (PML) nuclear bodies are disorganized in colorectal tumors with total loss of major histocompatibility complex class I expression and LMP7 downregulation. Tissue Antigens 2004;63:446–452.
26. Gurrieri C, Capodieci P, Bernardi R, et al. Loss of the tumor suppressor PML in human cancers of multiple histologic origins. J Natl Cancer Inst 2004;96:269–279.
27. Nguyen LA, Pandolfi PP, Aikawa Y, et al. Physical and functional link of the leukemia-associated factors AML1 and PML. Blood 2005;105:292–300.
28. Shitashige M, Satow R, Jigami T, et al. Traf2- and Nck-interacting kinase is essential for Wnt signaling and colorectal cancer growth. Cancer Res 2010;70:5024–5033.
29. Condemine W, Takahashi Y, Zhu J, et al. Characterization of endogenous human promyelocytic leukemia isoforms. Cancer Res 2006;66:6192–6198.
30. Jensen K, Shiels C, Freemont PS. PML protein isoforms and the RBCC/TRIM motif. Oncogene 2001;20:7223–7233.
31. Duprez E, Saurin AJ, Desterro JM, et al. SUMO-1 modification of the acute promyelocytic leukaemia protein PML: implications for nuclear localisation. J Cell Sci 1999;112:381–393.
32. Shen TH, Lin HK, Scaglioni PP, et al. The mechanisms of PML-nuclear body formation. Mol Cell 2006;24:331–339.
33. Gao C, Ho CC, Reineke E, et al. Histone deacetylase 7 promotes PML sumoylation and is essential for PML nuclear body formation. Mol Cell Biol 2008;28:5658–5667.
34. Tatham MH, Kim S, Jaffray E, et al. Unique binding interactions among Ubc9, SUMO and RanBP2 reveal a mechanism for SUMO paralog selection. Nat Struct Mol Biol 2005;12:67–74.
35. Saitoh N, Uchimura Y, Tachibana T, et al. In situ SUMOylation analysis reveals a modulatory role of RanBP2 in the nuclear rim and PML bodies. Exp Cell Res 2006;312:1418–1430.
36. Petrie K, Zelent A. Marked for death. Nat Cell Biol 2008;10:507–509.
37. Zhong S, Muller S, Ronchetti S, et al. Role of SUMO-1-modified PML in nuclear body formation. Blood 2000;95:2748–2752.
38. Fogal V, Gostissa M, Sandy P, et al. Regulation of p53 activity in nuclear bodies by a specific PML isoform. EMBO J 2000;19:6185–6195.
39. Zhu H, Wu L, Maki CG. MDM2 and promyelocytic leukemia antagonize each other through their direct interaction with p53. J Biol Chem 2003;278:49286–49292.
40. Bernardi R, Scaglioni PP, Bergmann S, et al. PML regulates p53 stability by sequestering Mdm2 to the nucleolus. Nat Cell Biol 2004;6:665–672.
41. Fu C, Ahmed K, Ding H, et al. Stabilization of PML nuclear localization by conjugation and oligomerization of SUMO-3. Oncogene 2005;24:5401–5413.
42. Ishov AM, Sotnikov AG, Negorev D, et al. PML is critical for ND10 formation and recruits the PML-interacting protein daxx to this nuclear structure when modified by SUMO-1. J Cell Biol 1999;147:221–234.
43. Lallemand-Breitenbach V, Jeanne M, Benhenda S, et al. Arsenic degrades PML or PML-RARalpha through a SUMO-triggered RNF4/ubiquitin-mediated pathway. Nat Cell Biol 2008;10:547–555.
44. Reineke EL, Lam M, Liu Q, et al. Degradation of the tumor suppressor PML by Pin1 contributes to the cancer phenotype of breast cancer MDA-MB-231 cells. Mol Cell Biol 2008;28:997–1006.
45. Korinek V, Barker N, Moerer P, et al. Depletion of epithelial stem-cell compartments in the small intestine of mice lacking Tcf-4. Nat Genet 1998;19:379–383.
46. Ito K, Bernardi R, Morotti A, et al. PML targeting eradicates quiescent leukaemia-initiating cells. Nature 2008;453:1072–1078.
47. Lallemand-Breitenbach V, Zhu J, Puvion F, et al. Role of promyelocytic leukemia (PML) sumolation in nuclear body formation, 11S proteasome recruitment, and As2O3-induced PML or PML/retinoic acid receptor alpha degradation. J Exp Med 2001;193:1361–1371.

Received April 7, 2011. Accepted November 25, 2011.

Reprint requests

Address requests for reprints to: Tesshi Yamada, MD, PhD, Division of Chemotherapy and Clinical Research, National Cancer Center Research Institute, 5-1-1 Tsukiji, Chuo-ku, Tokyo 104-0045, Japan. e-mail: tyamada@ncc.go.jp; fax: (81)3-3547-6045.

Acknowledgments

The authors thank Drs de Thé and Le Bras for provision of the anti–PML-IV antibody and Dr Wilson for providing pcDNA3.1-human Ubc9.

Conflicts of interest

The authors disclose no conflicts.

Funding

Supported by the Program for Promotion of Fundamental Studies in Health Sciences conducted by the National Institute of Biomedical Innovation of Japan and the Third-Term Comprehensive Control Research for Cancer and Research on Biological Markers for New Drug Development conducted by the Ministry of Health, Labor, and Welfare of Japan. These sponsors had no role in the design of the study, the collection of the data, the analysis and interpretation of the data, the decision to submit the manuscript for publication, or the writing of the manuscript.

UICC
global cancer control

IJC
International Journal of Cancer

Carcinogenetic risk estimation based on quantification of DNA methylation levels in liver tissue at the precancerous stage

Ryo Nagashio[1], Eri Arai[1], Hidenori Ojima[1], Tomoo Kosuge[2], Yutaka Kondo[3] and Yae Kanai[1]

[1] Pathology Division, National Cancer Center Research Institute, Tokyo, Japan
[2] Hepatobiliary and Pancreatic Surgery Division, National Cancer Center Hospital, Tokyo, Japan
[3] Division of Molecular Oncology, Aichi Cancer Center Research Institute, Nagoya, Japan

For appropriate surveillance of patients at the precancerous stage for hepatocellular carcinomas (HCCs), carcinogenetic risk estimation is advantageous. The aim of our study was to establish criteria for such estimation based on DNA methylation profiling. The DNA methylation status of 203 CpG sites on 25 bacterial artificial chromosome (BAC) clones, whose DNA methylation status had been proven to discriminate samples of noncancerous liver tissue obtained from patients with HCC (N) from normal liver tissue (C) samples by BAC array-based methylated CpG island amplification, was evaluated quantitatively using pyrosequencing. The 45 CpG sites whose DNA methylation levels differed significantly between C and N in the learning cohort (n = 22) were identified. The criteria combining DNA methylation status for the 30 regions including the 45 CpG sites were able to diagnose N as being at high risk of carcinogenesis with 100% sensitivity and specificity in the learning cohort and 95.6% sensitivity and 100% specificity in the validation (n = 90) cohort. DNA methylation status for the 30 regions in N samples was significantly correlated with the outcome of patients with HCCs, indicating that clinicopathologically valid DNA methylation alterations have already accumulated at the precancerous stage. The DNA methylation status of the 30 regions did not depend on the presence or absence of hepatitis virus infection, or the status of noncancerous liver tissue (chronic hepatitis or cirrhosis). These criteria may be applicable for carcinogenetic risk estimation using liver biopsy specimens obtained from patients who are followed up because of chronic liver diseases.

Hepatocellular carcinoma (HCC) is a common malignancy worldwide. Hepatitis virus infection is associated with an extremely high risk of HCC development. Although mass vaccination against hepatitis B virus (HBV) has been initiated, HBV-associated liver carcinogenesis will not be stamped out for many years, as the age at presentation of HBV is over 50 years mainly in Asia and Africa.[1] The spread of hepatitis C virus (HCV) in Japan that occurred in the 1950s and 1960s has resulted in a rapid increase in the incidence of HCC since 1980s.[2] In other countries, including the United States, HCV infection has spread more recently.[2] As HCC usually develops in liver already affected by chronic hepatitis or liver cirrhosis associated with hepatitis virus infection, the prognosis of patients with HCC is deemed poor, unless the cancer is diagnosed at an early stage. Therefore, surveillance at the precancerous stage will become a priority. In clinical practice, especially intensive surveillance should be performed on patients at high risk of HCC development, even if the patients are asymptomatic. Thus, risk estimation for HCC development is essential for the management of patients with chronic liver diseases.

Alterations of DNA methylation are among the most consistent epigenetic changes observed during multistage human carcinogenesis.[3,4] Accumulating evidence suggests that alterations of DNA methylation are involved even in the early and precancerous stages.[5,6] With respect to hepatocarcinogenesis, DNA methylation alterations associated with expression and/or splicing abnormalities of DNA methyltransferases are already present in liver tissues exhibiting chronic hepatitis or liver cirrhosis obtained from patients with HCCs.[7–11] Differing from alterations of mRNA and protein expression, which can be easily affected by the microenvironment of cancer

Key words: chronic hepatitis, hepatocellular carcinoma, liver cirrhosis, precancerous condition, pyrosequencing

Abbreviations: anti-HCV: anti-HCV antibody; BAC: bacterial artificial chromosome; BAMCA: BAC array-based methylated CpG island amplification; HBs-Ag: HBV surface antigen; HBV: hepatitis B virus; HCC: hepatocellular carcinoma; HCV: hepatitis C virus; PCR: polymerase chain reaction

Additional Supporting Information may be found in the online version of this article.

Grant sponsors: Third Term Comprehensive 10-Year Strategy for Cancer Control from the Ministry of Health, Labor and Welfare of Japan, Cancer Research from the Ministry of Health, Labor and Welfare of Japan, Program for Promotion of Fundamental Studies in Health Sciences of the National Institute of Biomedical Innovation (NiBio), Foundation for Promotion of Cancer Research in Japan

DOI: 10.1002/ijc.26061

History: Received 7 Oct 2010; Accepted 17 Feb 2011; Online 11 Mar 2011

Correspondence to: Yae Kanai, Pathology Division, National Cancer Center Research Institute, 5-1-1 Tsukiji, Chuo-ku, Tokyo 104-0045, Japan, Tel.: +81-3-3542-2511, Fax: +81-3-3248-2463, E-mail: ykanai@ncc.go.jp